To the Graduate Council:

I am submitting herewith a thesis written by Amol G. Bokil entitled "Texture Analysis Based Object Detection in Single and Multichannel Aerial Imagery." I have examined the final copy of this thesis for form and content and recommend that it be accepted in partial fulfillment of the requirements for the degree of Master of Science, with a major in Electrical Engineering.

Mohan M. Trivedi

Mohan M. Trivedi, Major Professor

We have read this thesis
and recommend its acceptance:

Donald W. Bouldin

Marshall Pace

Accepted for the Council:

Cunninkel

Vice Provost
and Dean of The Graduate School

STATEMENT OF PERMISSION TO USE

In presenting this thesis in partial fulfillment of the requirements for a Master's degree at The University of Tennessee, Knoxville, I agree that the Library shall make it available to borrowers under rules of the Library. Brief quotations from this thesis are allowable without special permission, provided that accurate acknowledgment of the source is made.

Permission for extensive quotation from or reproduction of this thesis may be granted by my major professor, or in his absence, by the Head of Interlibrary Services when, in the opinion of either, the proposed use of the material is for scholarly purposes. Any copying or use of the material in this thesis for financial gain shall not be allowed without my written permission.

Signature Andr B[illegible]

Date DEC 2ND 1988

TEXTURE ANALYSIS BASED OBJECT DETECTION IN SINGLE AND MULTI CHANNEL AERIAL IMAGERY

A Thesis

Presented for the

Master of Science Degree

The University of Tennessee, Knoxville

Amol G. Bokil

December 1988

DEDICATION

This thesis is dedicated to my parents, whose love and support has been the mainstay of my life and career. Without their encouragement projects such as these would never have been completed.

ACKNOWLEDGEMENTS

I wish to express my appreciation to my major advisor, Dr. M. M. Trivedi, for his support, advice, and patience during the course of this research. I would also like to thank Dr. D. W. Bouldin and Dr. M. O. Pace for serving on my committee and reviewing this thesis.

In the pursuit of this degree, I have also benefited along the way from the help of many fellow students. In particular, I wish to mention Chuxin Chen who helped me every time I found myself in a difficulty. Mourad Takla, Mishi Saravi, Kevin Barnett, George Mathai, Joe Spears, Arnulfo Perez, K. G. Viswanathan, Chandra, Hamed Sari-Sarraf, Raja Ghozi were some of the other sources of encouragement. Special thanks go to Janet Smith for proofreading and helping with the various aspects of this thesis. In addition, the help of several support staff is also very much appreciated.

This research was supported, in part, by the U.S. Army research grant number DAAK70-87-P2569 with Prof. Trivedi as the principal investigator.

Last, but not the least, I would like to thank my parents, my brother Anupam and my friend Priti for standing by me during this period of my graduate study.

ABSTRACT

Accurate and reliable detection of objects is an important component of an image interpretation system. Objects might appear against a wide variety of background regions and as such characteristic properties of the objects are sought. Texture analysis based approaches are powerful in such applications since texture is a property inherent to a region. A gray level co-occurrence (GLC) based texture analysis package useful for object detection and image segmentation is developed. Most of the techniques found in literature employ a supervised classification scheme, where the classifier is trained with a set of training samples. Unavailability of the training samples and the expense associated with it has forced researchers to explore other strategies. Cluster analysis is the technique suggested in this study. It provides a logical means to perform unsupervised classification in a d-dimensional space. Forward sequential search based measurement selection strategy and Mahalanobis distance classifier are the elements of the supervised classification scheme. K–means cluster analysis algorithm is the unsupervised counterpart. The main focus of this study is the application of these two techniques to aerial images. A high resolution multispectral urban scene image and a high resolution thermal infra-red channel image is used to study the performance of these two techniques. Resubstitution testing procedure is applied generally, while in the analysis of the thermal infra–red image jackknifing is also employed. Supervised statistical classification scheme

seemed to perform better than the cluster analysis based classification scheme. Investigation of multispectral texture analysis is the other issue addressed in this thesis. A gray level difference (GLD) based technique for multispectral texture analysis is studied. Alternate approaches based on the GLC and the GLD methods are proposed to perform texture analysis in multispectral images. Appending the measures from each of the channels and using them for the object detection task is the underlying idea of the approaches suggested here. In the analysis of multispectral imagery the techniques suggested in this study, performed better in object detection as well as image segmentation tasks. Also, in general the proposed GLC based technique yields better results as compared to the gray level difference based method. The results obtained in the case of the analysis of multispectral imagery are better than those obtained when analyzing a single channel of the image indicating the superiority of multispectral analysis approach over the single channel analysis strategy.

TABLE OF CONTENTS

CHAPTER PAGE

1. INTRODUCTION 1

2. OBJECT DETECTION IN AERIAL IMAGES: A REVIEW 6

2.1 Detection of Objects in Aerial Images 6

2.2 Texture Analysis Based Object Detection 9

3. OBJECT DETECTION BY TEXTURE ANALYSIS IN SINGLE CHANNEL IMAGERY 12

3.1 GLC Matrix and Measures 12

3.2 Algorithms for Object Detection and Image Segmentation 15

3.3 Equal Probability Quantization 16

3.4 Supervised Classification Strategy 17

3.4.1 Mahalanobis Distance Classifier 18

3.4.2 Forward Sequential Search Based Measurement Selection Strategy 19

3.5 Unsupervised Classification Strategy 22

3.5.1 Motivation to Perform Cluster Analysis 22

3.5.2 K-means Cluster Analysis Algorithm 23

4. TEXTURE ANALYSIS IN MULTISPECTRAL IMAGES . . 26

CHAPTER PAGE

4.1 Multispectral Texture 27

4.1.1 Multispectral Texture Analysis using Gray Level Difference Method 28

4.1.2 Multispectral Texture Analysis Using the GLC Method . 32

4.1.3 Extension to Three or More Channels 33

4.2 Simple Extensions for Texture Analysis in Multispectral Images . 35

4.2.1 GLC Based Technique for Texture Analysis in Multispectral Images 36

4.2.2 GLD Based Technique for Texture Analysis in Multispectral Images 37

5. OBJECT DETECTION IN HIGH RESOLUTION AERIAL IMAGES: EXPERIMENTAL EVALUATION 38

5.1 Experiments With Single Channel Imagery 38

5.1.1 Experiments Performed on a High Resolution Multispectral Urban Scene Image 44

5.1.2 Experiments Performed on a High Resolution Thermal Channel Image 69

5.2 Experiments With Multichannel Imagery 78

5.2.1 Gray Level Co-occurrence Method for Texture Analysis in Multispectral Images 89

5.2.2 Gray Level Difference Method for Texture Analysis in Multispectral Images 95

CHAPTER PAGE

5.2.3 A Comparison of GLC and GLD Methods 101

6. SUMMARY AND CONCLUSIONS 105

BIBLIOGRAPHY 110

VITA 114

LIST OF FIGURES

FIGURE PAGE

4.1 A 4×4 digital image having three gray levels (channel 1). 29

4.2 A 4×4 digital image having three gray levels (channel 2). 31

4.3 A 4×4 digital image having three gray levels (channel 3). 34

5.1 Channel 1 of the image – Visible range. 40

5.2 Channel 2 of the image – Thermal infra-red range. 41

5.3 Channel 3 of the image – Near infra-red range. 42

5.4 A flow chart of the typical sequence of operation. 104

LIST OF TABLES

TABLE		PAGE
5.1	Results Obtained Using the Supervised Statistical Classification Technique (Visible Range).	48
5.2	Results Obtained Using the Unsupervised Technique (Visible Range).	52
5.3	Results Obtained Using the Statistical Classification Technique (Thermal Infra-red Range).	56
5.4	Results Obtained Using the Unsupervised Technique (Thermal Infra-red Range).	58
5.5	Results Obtained Using the Statistical Classification Technique (Near Infra-red Range).	63
5.6	Results Obtained Using the Unsupervised Technique (Near Infra-red Range).	66
5.7	Performance of the System (Cluster Analysis Based Classification Scheme).	76
5.8	Performance of the System (Supervised Statistical Classification Scheme Employing Jackknifing Testing Procedure).	78
5.9	Probability of error of the Various Techniques Used for Object Detection in Multichannel Imagery.	82

TABLE PAGE

5.10 Probability of error of the Various Techniques Used for Image Segmentation in Multichannel Imagery. 88

5.11 Results Obtained Using the Statistical Classification Technique (GLC append). 93

5.12 Results Obtained Using the Unsupervised Technique (GLC append). 94

5.13 Results Obtained Using the Statistical Classification Technique (GLD append). 100

5.14 Results Obtained From the Unsupervised Technique (GLD append). 101

CHAPTER 1

INTRODUCTION

Computer vision has applications in a wide variety of real world problems ranging from medicine to complex industrial environments. It can be viewed as a process of automatic interpretation of a scene. The problem of object detection is vital for an image interpretation system. The object detection procedure is required to detect objects that might appear against a wide variety of background regions. Ideally, features which are characteristic of the objects and minimally sensitive to the background are sought [1]. Texture is a property inherent to a region and thus is a powerful tool to attack the above mentioned problem.

Image segmentation is an important and a difficult task in the analysis of images. A part of the segmentation problem is the object detection problem. In the analysis of images two broad types of regions are usually encountered. The first type is characterized by a distributed or a textured pattern, examples of which are forests, agricultural land etc. while the other type consists of unique patterns occuring in some well defined regions in the scene such as the airplanes, cars etc. The second type of regions are called objects and their detection in high resolution images forms an important part of this study. The need for such unique object detection tasks can arise in a variety of applications, however, only the remote sensing field application is considered here. This study is directed in the direction of the research performed by Trivedi *et al.* [1]. A gray level co-occurrence (GLC) based texture analysis package useful for image segmentation and object detection is developed. The various measures (introduced in the chapters that follow) that are generated are characteristic properties of the different regions and as such some combination of these measures successfully isolate the targets from the background. Forward sequential search based measurement selection strategy helps to pick up the set of measures that support the task of object detection. Mahalanobis distance classifier is used in this study to assign the samples to the appropriate classes. Resubstitution testing procedure is adopted here. In the analysis of a high resolution thermal infra–red channel image jackknifing testing procedure is also employed. This testing procedure was not used in all the cases because this was not the main focus of the study and the resubstitution technique is computationally cheaper and faster. The study reported by Trivedi *et al.* [1] required a training phase for measurement selection. One of the major problems under investigation is the minimization of supervision in performing image segmentation and object detection tasks. Cluster analysis forms the basis of the line of attack adopted here to reduce the reliance on training samples. It offers a logical means for " unsupervised " classification of data in a d-dimension space. K-Means cluster analysis procedure is used to discriminate objects from the background regions. The measures to be used are input to the system by the user. This is justified on the basis of some prior specific application domain information the user may have such as the directionality of patterns, important intersample spacing distance values associated with the object structure etc. The fact to be noted, however, is that this technique is different from the one employed by Trivedi *et al.*[1] since their technique required a forward sequential search to select the best set of measures and a statistical classifier to perform the classification.

The first image analyzed was a high resolution multispectral urban scene image incorporating the visible range, the thermal infra–red range, and the near ingra–red range. The second image was a high resolution thermal infra–red channel image. The three channels of the multispectral image were considered as sub–images when an attempt was made to study the techniques as applied to a single channel image. In each of the cases promising results were obtained.

Investigation of multispectral texture analysis is the other issue addressed in this thesis. Most of the texture analysis techniques found in literature deal with single channel images. The concept of texture is fairly well understood for single channel images, but multispectral texture is not yet a clear concept. An attempt is made here to discuss multispectral texture from a computational stand point. The approach adopted by Rosenfeld *et al.* [2] for the analysis of multispectral texture tries to address the issue of multispectral texture from a computational stand point. Simple approaches based on the GLC and the GLD methods are proposed for the analysis in multispectral images. The image used in the first part of the experiments was ideally suited for this kind of study since it was a multichannel image. Object detection was performed using the techniques suggested in this study and the technique proposed by Rosenfeld *et al.*. Image segmentation was then performed on the multispectral urban scene image using the different techniques discussed in this thesis. Finally, the technique proposed here which consists of appending the measures generated in each of the channels and utilizing the complete set to perform the detection task are studied in detail by considering all the three channels. All the images experimented with in this study were 512×512 in size.

The supervised classification technique seemed to do better in each experiment. In both the cases *i.e.* single and multichannel images, it yielded a 100% classification accuracy. The unsupervised technique did not fare bad either. It provided a 96.3% accuracy when analyzing the thermal channel image. This technique did not produce a 100% classification accuracy when individual analysis on each of the channels was being performed, but it did yield perfect classification results when the measures from all the channels were considered thus highlighting the superiority of the multispectral analysis approach over the analysis of a single channel. In the analysis of multispectral images the appending technique (suggested here) performed better every time. When analyzing the image using all the 3 channels the GLC based appending method performed better than the gray level difference based appending method.

The organization of this thesis is as follows. Chapter 2 discusses some of the work done in the field of analysis of aerial images. This is followed by a brief look at the various texture analysis approaches. The GLC matrix and the texture measures employed for object detection are introduced in Chapter 3. Various algorithms used in the texture analysis based object detection task such as equal probability quantization, cluster analysis, forward sequential search, Mahalanobis distance classifier, etc. are dealt with in this chapter. Chapter 4 contains the discussion regarding the analysis of multispectral texture. Chapter 5 contains the experiments, results and their evaluation. Summary and conclusions are included in Chapter 6 which also proposes some directions along which future research efforts can be concentrated.

CHAPTER 2

OBJECT DETECTION IN AERIAL IMAGES: A REVIEW

In this chapter some of the approaches adopted in the analysis of aerial images are discussed. This is followed by a brief look at the various texture analysis techniques.

It is interesting to note that inspite of the extensive research in the field, a unique definition for " *TEXTURE* " still escapes the minds of the researchers. Texture can, in general, be considered as a structure composed of a large number of ordered elements offering a global unitary impression to the observer [3].

2.1 Detection of Objects in Aerial Images

Development of a vision system for the analysis of aerial scenes is a complex task. Basically the properties of the objects are exploited in order to arrive at the " object vs. background " discrimination. Some of the properties taken into consideration are spectral, spatial and topographic.

This study is basically directed in the direction of the research performed by Trivedi *et al.* [1]. They performed unique object detection task in high resolution aerial images. Object detection methodologies should possess the following features: they should be insensitive to the backgrounds on which the objects might appear, the orientation of an object should not affect its detectability, as far as possible, the techniques should use a unified set of operators to analyze various levels of details. The technique proposed by them incorporated the above requirements. GLC based operators were used to extract relevant image properties. The results underlined the importance of such operators in the analysis of high resolution aerial images. The operators used are early vision operators and thus did not require any semantic knowledge about the scene. The technique discussed required a training phase wherein the classifier was trained with a set of training samples and then tested with a set of test samples. Jackknife testing procedure was employed.

Another study performed by Trivedi *et al.* [4] illustrated the importance of GLC based operators in the task of object detection. Here again the classifier needed to be trained before it could be tested. Forward sequential search based measurement selection strategy was employed to select the best set of measures and the classifier was tested using those measures. Various experiments were performed. Objects appearing on a single background with arbitrary orientations as well as those appearing on a variety of backgrounds with arbitrary orientations were successfully detected. A series of decision modules were required to detect objects irrespective of their orientations.

In this study an attempt is being made to develop extensions to the above two studies with emphasis on reducing the training phase or supervision. This is required when the availability of training samples is scarce, which is indeed the situation in real life cases. Following are some of the attempts made by the researchers to overcome the training phase requirements in the analysis of aerial images.

Trivedi *et al.* [5] used spectral and spatial domain information to detect objects in high resolution multispectral aerial images. A hierarchical approach was used where object detection was accomplished by eliminating competing background regions based upon various spectral and spatial properties, in a step-wise manner. The processing steps consisted of noise suppression and enhancement of object like regions, followed by spectral information processing where the object like regions were identified based upon their spectral response. This was followed by spatial attribute matching, where the size, shape, and other spatial domain attributes were utilized to retain the most probable object regions for further processing. The last step – intensity profile matching – was inspired by the success GLCs had encountered. The intensity profiles of the object like regions were reconstructed using a fourth order polynomial. The analysis of the geometric shape represented by the polynomial is mathematically developed in reference [6]. The investigation of intensity profiles, finally, completed the discrimination task.

An approach similar to [5] was employed by Trivedi and Chen [7] to perform object detection by step-wise analysis of spatial, spectral, and topographic features. As the spectral information processing step, segmentation of a single channel image (using threshold) was performed and then the data from the remaining channels was analyzed using cluster analysis. Details of the threshold selection procedure that utilized a priori knowledge of object attributes can be found in reference [7]. A procedure to find the direction of the principal axis was also discussed. This is needed to determine the orientation of the region in the image in order to be able to calculate the spatial domain features like length, width etc.

From the above studies it can be seen that unsupervised techniques have been successfully used in the analysis of aerial images. In this study the unsupervised technqiue is experimented with in the domain of the GLC's. This kind of study is yet to be reported in literature where the measures generated from the GLC matrices are used to perform unsupervised classification of the samples.

2.2 Texture Analysis Based Object Detection

Several texture analysis approaches are presently being used. These can be broadly classified into two categories :

1. Statistical.

2. Structural.

Dewaele *et al.* [8] performed texture inspection with self-adaptive convolution filters. The size of the "sparse" convolution mask was determined by estimating the period in horizontal and vertical directions. A max-min measure for image texture analysis was described by Mitchell *et al.* [9]. This method essentially, was the determination of the number of local gray level maxima and minima along a one-dimensional scan direction. Syntactic and Structural approaches have been the mainstay of many a research efforts. Chong [10] performed a structural analysis of periodic and almost periodic textures. The approach consisted of determining periodicity using the *inertia* measure and from the *inertia* spectrum deriving two unit vectors that define the shape, size, and orientation of a period parallelogram unit pattern of the texture. Further, methods gauging uniformity and proximity, for detecting edges, and detecting corners were also presented. A complete discussion of the various texture analysis techniques can be found in reference [3]. Texture operators have been used widely in the analysis of aerial scenes [1,4,11,12].

The gray level co-occurrence (GLC) matrix and the measures derived from them have been used for a wide variety of applications. Carpet wear assessment [13], analysis of multi-resolution images [14], and object detection in aerial images [1,4,11,12] are some of the popular applications.

A GLC based package useful for object detection and image segmentation is developed as a first step in this research. The choice of this technique is underlined by the success it has encountered when applied to a host of real life problems. A comparison study performed by Weszka *et al.* [15] and Conners *et al.* [16] showed that the gray level co-occurrence method is more powerful than some of the other texture analysis techniques. As will be seen, the GLC matrix is a second order probability distribution (distribution of the gray levels). Julesz has pointed out the sensitivity of human beings to the second order statistics, which favors the use of GLC matrices. Periodicity detection has been accomplished using the measures derived from the GLC matrices. Conners and Harlow [17] have shown that the *inertia* measure can be used to characterize the placement rules and the unit pattern of periodic texture. Conners *et al.* [11] have presented strong evidence to conclude that no known example of a visually distinct texture pair exists which cannot be discriminated by the co-occurrence matrices. Thus, GLC matrices present a strong case for their utilization.

The various texture analysis techniques discussed so far have dealt with single channel images rather than multi channel or color images. Rosenfeld *et al.*[2] discussed the extension of two techniques to multispectral images. The computational difficulty and the expensive memory storage requirements prevented the use of the GLC method for multispectral images. Instead, the distribution of absolute differences of pairs of gray levels was utilized by them. They demonstrated that multispectral features yield better separations between texture classes than single-band features. The experiments were conducted on two-band data sets.

In the next chapter, the GLC matrix and the measures used for object detection and image segmentation are introduced. The implementation details of various algorithms used in the texture analysis based object detection task are also discussed.

CHAPTER 3

OBJECT DETECTION BY TEXTURE ANALYSIS IN SINGLE CHANNEL IMAGERY

The GLC matrix and the first and second order measures used in the process of object detection are introduced. Various algorithms that play a major role in the task of object detection and image segmentation are then discussed in this chapter. The concepts are discussed with single channel images in mind and can be extended to multi-channel images without much modification.

3.1 GLC Matrix and Measures

A GLC matrix $S(\delta, T) = [s(i, j, \delta, T)]$ is a matrix of estimated second order probabilities in which each element $s(i, j, \delta, T)$ is the estimated probability of going from gray level i to gray level j, given the displacement vector $\delta = (\Delta x, \Delta y)$ and T, the region size and shape used to estimate the probabilities. It is convenient to consider $\delta = (\Delta x, \Delta y)$ not in a cartesian form but rather in a polar form $\delta = (d, \theta)$ where $d = max(\Delta x, \Delta y)$ and $\theta = \arctan(\Delta x, \Delta y)$. In this form d is called the intersample spacing distance and θ is called the angular orientation

[1,4,11]. Computationally, $S(\delta, T)$ is calculated as :

$$s(i,j,\delta,T) = \frac{\mathbf{O}[x|x, x+\delta\epsilon\sigma(T), g(x)=i, g(x+\delta)=j]}{\mathbf{N}}$$

where $\mathbf{O}$ denotes the order of the set *i.e* the number of elements;

$$\mathbf{N} = \mathbf{O}[x|x, x+\delta\epsilon T]$$

σ is a function called isometry transformation; and $g(x)$ is the picture function [1,4,12].

Haralick *et al.* [18] defined a set of measures to extract useful textual information from the GLC matrix. It was reported by Conners *et al.* [16] that these measures did not contain all the important texture-context information and thus two new measures surfaced as a result of extensive research. The measures used in this research effort were inertia, energy, entropy, local homogeneity, cluster shade and cluster prominence. These measures have proven to be very powerful in the process of object detection [1,4,11]. They are defined as follows,

1. Inertia:

$$I(\delta,T) = \sum_{i=0}^{L-1}\sum_{j=0}^{L-1}(i-j)^2 s(i,j,\delta,T),$$

2. Energy:

$$E(\delta,T) = \sum_{i=0}^{L-1}\sum_{j=0}^{L-1}(s(i,j,\delta,T))^2,$$

3. Entropy:

$$H(\delta,T) = -\sum_{i=0}^{L-1}\sum_{j=0}^{L-1} s(i,j,\delta,T)\log s(i,j,\delta,T),$$

4. Local Homogeneity:

$$L(\delta, T) = \sum_{i=0}^{L-1} \sum_{j=0}^{L-1} \frac{1}{1+(i-j)^2} s(i,j,\delta,T),$$

5. Cluster Shade:

$$A(\delta, T) = \sum_{i=0}^{L-1} \sum_{j=0}^{L-1} (i+j-\mu_x-\mu_y)^3 s(i,j,\delta,T),$$

6. Cluster Prominence:

$$B(\delta, T) = \sum_{i=0}^{L-1} \sum_{j=0}^{L-1} (i+j-\mu_x-\mu_y)^4 s(i,j,\delta,T),$$

where,

$$\mu_x = \sum_{i=0}^{L-1} i \sum_{j=0}^{L-1} s(i,j,\delta,T),$$

$$\mu_y = \sum_{i=0}^{L-1} \sum_{j=0}^{L-1} j s(i,j,\delta,T),$$

and L is the number of gray levels in the processed image [1,11].

In addition to the second order measures described above, two first order measures were also considered [19],

1. Mean:

$$m = \frac{1}{N} \sum_{i=1}^{N} x_i$$

2. Variance:

$$v = \frac{1}{N} \sum_{i=1}^{N} x_i x_i' - m_i m_i'$$

These measures, for different combinations of d and θ, formed the data set for our study.

3.2 Algorithms for Object Detection and Image Segmentation

First, the overall sequence of processing is discussed following which the details of each of the processing steps are presented. The image is first subjected to the process of equal probability quantization. This is done to remove the effects of brightness and contrast variations that might otherwise dominate the measured feature values. A reduction in the number of gray levels is also achieved effectively using this technique. Once this is done, the first and the second order measures are generated from the equal probability quantized image for all values of δ, and for each sample. From large measurement sets, as the ones encountered here, a smaller set of measures needs to be selected that yields a minimum probability of error. The technique adopted in this study is the forward sequential search based measurement selection. A statistical classifier *i.e* Mahalanobis distance classifier is utilized to classify the samples using the measures presented by the measurement selection algorithm. The forward sequential search algorithm along with the Mahalanobis distance classifier forms the supervised classification technique where the classifier is first trained with a set of samples and then tested. In real life cases, the availability of training samples is quite limited and thus the supervised classification scheme is not applicable. This drawback underlines the need for an unsupervised classification scheme. Cluster analysis is the technique adopted here. Specifically, K-means algorithm is used which is an approach based on the optimization of an objective function and thus provides a well-defined approach to cluster analysis.

3.3 Equal Probability Quantization

Equal probability quantization has been a preprocessing step in image processing problems for a long time. Its importance in texture analysis has been repeatedly stressed [2,4,15,20]. Conners and Harlow [20,21] have shown through a series of experiments that this process has two basic properties which makes it an important step in texture analysis tasks.

1. It can be used to "normalize" the image contrast.

2. It provides an optimal way to reduce the number of gray levels in the image and yet retain an accurate representation of the image.

They state that equal probability quantization successfully removes effects of contrast variations caused by the differences in the scanning parameters, on the texture measures computed from the gray level co-occurrence (GLC) matrices. This is extremely necessary in real life cases. Texture measures computed from an image acquired under different scanning parameter settings should essentially be the same and not be a function of the scanning parameters. Contrast sensitivity of many texture analysis algorithms led Haralick *et al.* [18] to introduce the concept of equal probability quantization, which is referred to in literature as "Histogram flattening". The algorithm employed in this study is the one developed by Conners *et al.* [21] which differs slightly from the one proposed by

Haralick [18] in the initializing step.

A reduction in the number of gray levels is required in many image analysis applications. One approach to this is to linearly redistribute the gray levels in the image such that they are equally spaced. This leads to some gray levels being used to the fullest extent while others being under utilized. Equal probability quantization guarantees that all the gray levels, in the desired range, have an equal probability of occurrence and thus no gray levels are under utilized. Measures computed from linearly reduced images vary significantly with changes in the scanning parameters which is not the case with the images reduced by equal probability quantization. Conners and Harlow [21] performed a large set of experiments before concluding the above statement. Equal probability quantization serves as a preprocessing step for other texture analysis algorithms like gray level run method and gray level difference method. A detail development of this algorithm can be found in reference [21].

3.4 Supervised Classification Strategy

The forward sequential search based measurement selection strategy and the statistical classifier - Mahalanobis distance classifier, are the elements of the supervised classification scheme. As indicated earlier, this process requires a set of labelled samples to train the classifier which is then tested with the set of test samples. The measures to be used for classification are provided by the forward sequential search algorithm which is the measurement selection strategy and the classification is performed by the Mahalanobis distance classifier. This scheme is based on the assumption that the measurement vectors computed from the regions containing the objects, form a compact cluster defined by the normal density function, $N(\mu, \Sigma)$, while the vectors computed from the background regions lie away from this cluster. The measurement selection strategy assures that such is indeed the case. This technique has been a mainstay of many a research efforts [1,4,11]. The Mahalanobis distance classifier and the forward sequential search based measurement selection strategy are discussed next.

3.4.1 Mahalanobis Distance Classifier

Given the normality assumption, it becomes clear that for a sample to belong to a class it should be at a distance less than a certain threshold, from the distribution of the class. Mahalanobis distance between a measurement vector $\underline{X}$ and $\underline{\mu}$, the mean of the object class is computed as

$$(\underline{X} - \underline{\mu})^T \Sigma^{-1} (\underline{X} - \underline{\mu}),$$

where Σ is the covariance matrix.

This is a variation of Chi–squared test and has been developed in reference [4]. Given a normality assumption a Chi–squared procedure can be used to determine whether the n–dimensional vector $\underline{X}$ is a member of $N(\mu, \Sigma)$ with α degree of certainty. In particular, the H_0 hypothesis is considered true if

$$(\underline{X} - \underline{\mu})^T \Sigma^{-1} (\underline{X} - \underline{\mu}) \leq T = X^2_{\alpha,n},$$

where $X^2_{\alpha,n}$ is 100α percentage point of the Chi–squared distribution, otherwise accept H_1. The left hand side of the above equation is the squared Mahalanobis distance, which in a way indicates the membership of a sample to a given class. This distance, if large, is indicative of the fact that the sample does not belong to the object class. To define "large", a threshold needs to be robustly selected. The Mahalanobis distances of all the samples is compared with a threshold T and a sample is assigned to the object class, if its distance is less than T, else it is assigned to the background class.

3.4.2 Forward Sequential Search Based Measurement Selection Strategy

The second and the first order measures together form the complete set of measures. Obviously one is dealing with a large set of measures and thus it becomes critical to have a robust technique that will select the *best* set of measures from all the available measures. A measurement selection procedure based on the forward sequential search is discussed, the development of which can be found in reference [4]. The "best" set of measures means, the set that provides the best performance *i.e* the smallest emperically evaluated probability of error. The probability of error (POE) is computed by taking into account the misses (targets called backgrounds) and the false-alarms (backgrounds called targets). Computationally, the probability of error is computed as

$$POE = \frac{\text{number of misses} + \text{number of false-alarms}}{\text{total number of samples}}$$

The measurement selection process also yields an optimal threshold which can be used in the process of object detection. The forward sequential search algorithm is discussed below.

Let m be the number of measures available. The problem is to select n measures out of the m available measures ($n << m$), such that these measures provide the smallest probability of error. This procedure utilizes the Mahalanobis distance classifier. This classifier performs the classification by comparing the Mahalanobis distances of each sample with a threshold and assigning the samples to the appropriate classes.

The algorithm can be considered as a two step process. Let $\underline{X} = \{X_1, X_2, ..., X_m\}$ be the set of available measures.

<u>**Step 1:**</u> Selection of the first measure;

Let $i = 1$.

1. Select X_i^{th} measure of the set.

2. Design the Mahalanobis distance classifier.

3. Test this classifier with the test data, *i.e* compare the Mahalanobis distances of all the samples with a threshold T and assign a sample to the object class if its Mahalanobis distance is less than T, else assign it to the background class. This is done for a set of values of T and the threshold that yields the minimum probability of error is noted as the optimal threshold.

4. Note $(POE)_{X_i}$.

5. Set $i = i + 1$, go back to 1 if $i < m$.

Finally, determine j such that $(POE)_{X_j}$ is the smallest.

Step 2: Selection of a $2 - d$ measurement set;

1. Select (X_j, X_i) such that $X_i = X_p$ if $X_j \neq X_p$.

2. Design $2 - d$ Mahalanobis distance classifier.

3. Test this classifier with the test data and note the $(POE)_{X_j X_i}$.

4. Set $i = i + 1$, go back to 1 if $i < m$.

Finally, determine k such that $(POE)_{X_i X_k}$ is the smallest.

Similar technique is adopted for a measurement set with $n > 2$. This algorithm terminates when any of the following criteria are satisfied.

1. If the prescribed number (n) of measures are selected.

2. If $n = m$, *i.e* all the measures are selected.

3. If $(POE)_{k+1} \geq (POE)_k$, *i.e* augmenting another measure to the set of measures at the k^{th} iteration deteriorates the performance of the classifier.

As is obvious, the algorithm involves a training phase wherein the classifier is trained *i.e* μ, Σ, and T are estimated, and then asked to do the classification. Minimization of supervision in the object detection task is the issue being considered and the motivation to have such a technique is discussed next.

3.5 Unsupervised Classification Strategy

In this section the motivation to perform cluster analysis is first highlighted and then the clustering algorithm adopted here is discussed.

3.5.1 Motivation to Perform Cluster Analysis

The measurement selection strategy and the classifier discussed above required the availability of training samples for the design of the classifier. Such a procedure where training samples are employed is said to be *supervised*. The need for an *unsupervised* procedure arises from the fact that availability of training samples is quite limited in real life cases and the collection and labelling of samples can be costly and time consuming. Consider the example of missiles, which are extremely costly to be used for training a classifier. In such cases the supervised technique falls short of its expectations and the unsupervised technique comes to the rescue. The studies performed in [1,4,11] use the supervised technique and as such the question of getting around this phase arises. Cluster analysis is the approach adopted in this study. Clustering the data set into subgroups or clusters offers a logical means for unsupervised classification in R^d. A number of clustering techniques exist today and have become to be among the more useful tools for pattern recognition tasks. Trivedi *et al.* [22] performed segmentation of aerial images using fuzzy clustering concepts. A detailed discussion of unsupervised classification can be found in reference [23].

3.5.2 K-means Cluster Analysis Algorithm

Suppose $N = \{X_1, X_2, ..., X_n\}$ is a set of n samples to be clustered in c clusters. Many simple intuitive procedures exist [19] which can do the needful. A more well defined approach is to define a criterion (objective) function that measures the *goodness* of the partition in quantitative terms. The problem then becomes one of determining the partition that optimizes the criterion function. The objective function selected for this study is a measure of error incurred by representing individual pattern vectors by the prototype associated with them. Mathematically,

$$J_i = \sum_{k=1}^{N} \|\underline{X}_k - \underline{V}_i\|^2,$$

where $\underline{X}_k$ is a sample belonging to class i. $\underline{V}_i$ is the prototype of class i. It can be shown that the cluster center which minimizes this objective function is the sample mean

$$\underline{V} = \frac{1}{N} \sum_{j=1}^{N} \underline{X}_j.$$

The algorithm that utilizes this idea is the K-means algorithm. Studies have indicated that the K-means algorithm is in practice quite feasible in analyzing aerial images. The algorithm can be stated as follows [24].

1. Choose K initial clusters.

2. At the k^{th} iteration step distribute the samples among the K clusters using the 1-Nearest Prototype rule *viz.*

$\underline{X} \epsilon S_j(K)$ if

$$\|\underline{X} - \underline{V}_j(K)\| < \|\underline{X} - \underline{V}_i(K)\|$$

$\forall i \neq j$. Ties resolved arbitrarily.

3. Compute the cluster centers of the clusters thus formed.

$$\underline{V}_j(K+1) = \frac{1}{N_j} \sum_{X \epsilon S_j(K)} \underline{X},$$

   where $j = 1, 2, ..., K$. N_j is the number of samples belonging to class j.

4. If $\|\underline{V}_j(K+1) - \underline{V}_j(K)\| \leq \epsilon$ then terminate

   else go to step 2.

As can be anticipated, application of this algorithm to practical cases requires experimenting with different values of K and different starting strategies.

The clusters formed are usually represented as membership matrices. Let V_{cn} be the set of real $(c \times n)$ matrices where c is the number of classes and n is the number of samples. Then the membership matrix is defined as

$$M_c = \{U \epsilon V_{cn} \mid U_{ik} \epsilon \{0, 1\} \forall i, k; \sum_{k=1}^{n} U_{ik} > 0 \forall i, \sum_{i=1}^{c} U_{ik} = 1 \forall k\}$$

which indicates that a sample can belong to one class only and a class can have more than one sample and in fact no class can be without a sample.

In summary, the supervised technique which involves the forward sequential search and the Mahalanobis distance classifier, and the unsupervised technique involving the K-means clustering algorithm to which the measures are input by the user, offer two alternate ways of analyzing images for the task of object detection.

CHAPTER 4

TEXTURE ANALYSIS IN MULTISPECTRAL IMAGES

The texture analysis techniques discussed so far have been and are being used on single channel images. Texture measures computed from the samples belonging to one class form a compact cluster far away from the one formed by the samples of another class, thus aiding in the task of object discrimination. The question that immediately comes to the mind is how can this technique be utilized in case of multispectral images? This is the issue being addressed here.

Satellite and airborne multispectral scanners provide images of the same area of the Earth's surface as seen through different spectral bands [24]. The number of bands vary usually form four, as in LANDSAT images [22] to 20 or more for many aircraft borne scanners [24]. Various objects appear different in different channels, those darker in one channel might appear brighter in some other channel and so on. The image used in this study was a three channel image incorporating the visible, thermal infra-red, and near infra-red bands. It is definitely a matter worth pondering about as to how the object detection task can be accomplished using textures in such cases. Color images have three separate components – red, blue, and green. Texture analysis of such images also needs to be investigated.

In this chapter the concept of multispectral texture is discussed first. This is followed by a discussion of the approach adopted by Rosenfeld *et al.*[2]. Finally, an alternate approach is suggested to perform texture analysis in multispectral images.

4.1 Multispectral Texture

One reason for the relatively less work done in this field is the difficulty associated with acquiring multispectral images. Multispectral scanners are very expensive and as such its use has been typically in certain military and environmental monitoring studies.

With very little help from the literature, it is difficult to visualize, conceptually the meaning of multispectral texture. In single channel imagery texture is fairly well understood, but in multispectral images, the texture present in all the channels has to be collectively addressed. In this thesis, multispectral texture is discussed from the computational stand point. The technique adopted by Rosenfeld *et al.*[2] is an attempt to infer certain qualitative observations that could not be arrived at by analyzing the different bands separately. This approach is disussed next.

Rosenfeld *et al.* [2] discussed the extension of two techniques presently being used for single channel images. They are:

1. Gray Level Difference Method, and

2. Gray Level Co-occurrence (GLC) Method.

These techniques as applied to multispectral texture analysis are discussed below.

4.1.1 Multispectral Texture Analysis using Gray Level Difference Method

It has been shown that the gray level difference method performs as well as the GLC method for some texture classification tasks [15]. In the case of single channel images the gray level difference distribution is represented as a difference histogram. It is a vector with dimensionality n, where n is the number of gray levels in the image,

$$(a, b, c, ...)_n,$$

and the k^{th} element indicates the number of pairs of pixels, for a given δ, that have a gray level difference (absolute) k.

The above computation can be illustrated with a simple example. A 4×4 digital image having three gray levels is shown in Fig. 4.1.

The difference histogram for $\delta = (1,0)$ is $(4,6,2)$. It is interesting to note that the difference histogram can be obtained from the corresponding gray level co-occurrence matrix too. The GLC matrix for the image shown in Fig. 4.1, for

1	2	0	1
1	1	2	0
2	1	2	2
0	0	1	1

Figure 4.1: A 4×4 digital image having three gray levels (channel 1).

$\delta = (1, 0)$ is

$$\frac{1}{12}\begin{pmatrix} 1 & 2 & 0 \\ 0 & 2 & 3 \\ 2 & 1 & 1 \end{pmatrix}.$$

Summing the elements along the main diagonal yields the number of pairs of pixels differing in their gray levels by zero, which is the first entry in the difference histogram. By adding the elements along lines parallel to the main diagonal we obtain a signed difference histogram and not an absolute difference histogram. To obtain an absolute difference histogram the matrix needs to be made symmetric by adding pairs of elements symmetric with respect to the main diagonal and then summing the elements parallel to the main diagonal in the upper triangle alone gives the absolute difference histogram. The upper triangle is depicted below,

$$\begin{matrix} 1 & 2 & 2 \\ & 2 & 4 \\ & & 1 \end{matrix}$$

The normalizing factor that is present in the GLC matrix is not considered while computing the difference histogram from the GLC matrix.

Several measures can be computed from the difference histograms which can be used in the task of object detection. The measures used in this study are defined as follows [15],

1. Contrast:

$$CON = \sum_{i=0}^{L-1} i^2 p_\delta(i),$$

2. Angular second moment:

$$ASM = \sum_{i=0}^{L-1} p_\delta(i)^2,$$

3. Entropy:

$$ENT = -\sum_{i=0}^{L-1} p_\delta(i) \log p_\delta(i),$$

4. Mean:

$$Mean = \frac{1}{L} \sum_{i=0}^{L-1} p_\delta(i),$$

5. Inverse difference moment:

$$IDM = \sum_{i=0}^{L-1} \frac{p_\delta(i)}{i^2+1},$$

where $p_\delta(i)$ is a member of the difference histogram indicating the number of pairs of pixels have an absolute difference i for a given δ, and L is the number of gray levels in the image. The measures, as is evident, are analogous to those defined on the GLC matrix.

Rosenfeld *et al.* [2] extended this technique to two band images. Here the gray level difference distribution indicates how often a pair (difference in band 1, difference in band 2) occurs for a given δ. This can be better understood with the help of an example. Let Fig. 4.1 depict channel 1 and let Fig. 4.2 represent channel 2.

2	2	0	2
0	0	2	1
1	0	1	1
2	0	0	2

Figure 4.2: A 4×4 digital image having three gray levels (channel 2).

Thus, the two channel difference histogram for $\delta = (1, 0)$ is

$$(0,0) = 2 \qquad (0,1) = 0 \qquad (0,2) = 2$$

$$(1,0) = 2 \qquad (1,1) = 2 \qquad (1,2) = 2$$

$$(2,0) = 0 \qquad (2,1) = 1 \qquad (2,2) = 1$$

The entry $(0,0) = 2$ indicates that ther are two pairs of pixels that have the absolute difference vector $(0,0)$ *i.e* difference is 0 in the first channel as well as the second channel. As can be noted, it is a 2-dimensional $n \times n$ array, where n is the number of gray levels. The size of the difference histogram varies with the number of gray levels (n) and the number of bands (b) as n^b [2].

From the difference histogram several measures can be computed which can be used for the task of texture classification. Some of the measures are defined as follows :

1. Angular Second Moment (ASM):

$$ASM = \sum_{i=0}^{L-1} \sum_{j=0}^{L-1} e_{ij}^2,$$

2. Contrast (CON):

$$CON = \sum_{i=0}^{L-1} \sum_{j=0}^{L-1} e_{ij}(i-j)^2,$$

3. Inverse Difference Moment (IDM):

$$IDM = \sum_{i=0}^{L-1} \sum_{j=0}^{L-1} \frac{e_{ij}}{1+(i-j)^2},$$

where e_{ij} is an element of the difference histogram having gray level difference i in the first band and j in the second and L is the number of gray levels in the image.

4.1.2 Multispectral Texture Analysis Using the GLC Method

The GLC method for single channel images has been discussed in the earlier chapters. This concept can be generalized to any number of channels, but as will be observed, the computational complexity increases as the number of channels and the number of gray levels increase.

A GLC matrix, in case of a single channel image, indicates how often a particular pair of gray levels occurs in an image for a given δ. Its extension to two channels is best understood from the following illustration.

Let us consider the same images as before *i.e*, Fig. 4.1 and Fig. 4.2. For $\delta = (1,0)$, the GLC matrix for channel 1 is

$$\frac{1}{12}\begin{pmatrix} 1 & 2 & 0 \\ 0 & 2 & 3 \\ 2 & 1 & 1 \end{pmatrix}.$$

The GLC matrix for channel 2 is

$$\frac{1}{12}\begin{pmatrix} 2 & 1 & 3 \\ 1 & 1 & 0 \\ 2 & 1 & 1 \end{pmatrix}.$$

For a two band image, the array will be 4-dimensional whose $(i_1, i_2, i_3, i_4)^{th}$ element is the number of pixel pairs having gray levels (i_1, i_2) in the first band and the pair (i_3, i_4) in the second band, for a given δ. This array, therefore, has 81 elements. As the number of gray levels increase, the number of elements in the array increase underlining the need for expensive storage space. The size of the array grows with an increase in the number of gray levels (n) and the number of channels (b) as n^{2b} [2].

4.1.3 Extension to Three or More Channels

The GLC method can become very tedious as the number of channels increase. To illustrate this, consider the two previous images as two channels of an image and let Fig. 4.3 be the third channel of the image.

2	0	1	2
2	2	1	0
2	0	1	2
1	0	2	0

Figure 4.3: A 4×4 digital image having three gray levels (channel 3).

For $\delta = (1,0)$ the GLC matrix for channel 3 is

$$\frac{1}{12}\begin{pmatrix} 0 & 2 & 1 \\ 2 & 0 & 2 \\ 3 & 1 & 1 \end{pmatrix}.$$

The three-band analog of the co-occurrence matrix is 6-dimensional and the number of elements 3^6, *i.e* 729. Now, if the number of gray levels increase, the storage requirements rise drastically making this technique inefficient for three or more channels.

The gray level difference method is somewhat more manageable. The difference histogram for the image in Fig. 4.3 is $(1,7,4)$ for $\delta = (1,0)$. The three channel difference histogram is

$$(0,0,0) = 1$$

$$(0,0,1) = 1$$

$$(0,0,2) = 0$$

$$(0,1,0) = 0$$

$$(0,1,1) = 0$$

and so on. The array is thus, 3-dimensional and the number of elements $3^3 = 27$. This technique, though more practical than the GLC method, encounters difficulties when the number of gray levels in the image is large.

4.2 Simple Extensions for Texture Analysis in Multispectral Images

The two techniques discussed, pose several problems when dealing with real life cases where the number of gray levels in the image is much greater than three. In this study the number of gray levels was reduced from 256 to 16 for all the channels of the multichannel image. The number of elements in the difference histogram array would then be, 16^3 for the GLD method and 16^6 for the GLC method. A look at these numbers and the need for an alternate practical technique is obvious.

The problem, to which a solution is being sought is that of object detection using texture analysis. Rosenfeld *et al.* [2] attempted to address the issue of multispectral texture – where texture in all the channels need to be collectively considered. The methods they proposed become impractical when images having greater than two channels are being considered. The number of gray levels in the image also influences the size of the difference histogram array. With these shortcomings in view, alternative techniques need to be thought of to solve the mentioned problem.

The different channels of the image can be treated independently and the measures generated from them. Now, each of these channels have their textural characteristics embedded in the measures generated. All these measures can be considered as a single set of measures and used for the task of object detection. Objects appear different in different channels and as such those not easily identifible in one channel might, in fact, be so in some other channel. This feature can be made use of by utilizing measures from all the channels. Classification techniques may not yield perfect classification using the measures for individual channels, but for some combination of measures from all the channels, a perfect classification can result. The classification techniques have a larger set of measures to choose from as compared to the measures of a single channel only. It should be noted that this is not multispectral texture analysis but is the texture analysis in multispectral images. This is an attempt where an approximation to the multispectral texture analysis is sought. The idea of using as much information as possible from the available sources and the need for a computationally practical technique form the basis of this approach. Two specific approaches based on this technique are described below.

4.2.1 GLC Based Technique for Texture Analysis in Multispectral Images

Each channel is treated as though it is an independent image, *i.e* the GLC matrices and the texture measures are generated for each channel of the image separately. The measures from the three channels are appended for each of the samples. All these measures are then fed to the forward sequential search algorithm which comes up with the best set of features to be used for classification. This larger domain of measures gives the forward sequential search algorithm more number of measures to choose from. This set of measures is also experimented with in the unsupervised classification domain. This technique is compared with the individual analysis of the channels and the results are illustrated in chapter five which deals with the results.

4.2.2 GLD Based Technique for Texture Analysis in Multispectral Images

The same procedure described above is followed. The difference histograms are generated from the channels independently, the measures computed, appended and the entire set of measures is forwarded to the forward sequential search algorithm. Unsupervised technique is also studied using these measures.

Finally, a comparison of the two techniques is performed and the results are tabulated in the next chapter which deals with the experiments performed and the results.

CHAPTER 5

OBJECT DETECTION IN HIGH RESOLUTION AERIAL IMAGES: EXPERIMENTAL EVALUATION

In the previous two chapters, object detection approaches for single and multi–channel images were described and developed. In this chapter, the experimental studies undertaken are described. It is important that the techniques proposed in theory be feasible in practice and as such the approaches discussed so far are verified on real images. Experiments performed on single channel images are discussed first. Following these, the experiments performed on multichannel images are presented. A comparative evaluation of the techniques is included wherever appropriate.

5.1 Experiments With Single Channel Imagery

Two sets of experiments were performed in this category. The first image analyzed was a high resolution multichannel urban scene image. Since an attempt was being made to study the supervised statistical classification and the cluster analysis based (unsupervised) classification techniques as applied to single channel imagery, the different channels were considered as subimages and dealt with independently. This image was acquired by a multispectral scanner that could scan in 13 different spectral bands at a time. The three channels used here were – visible, thermal infra-red, and near infra-red. This image provided a variety of classes from which the samples could be chosen. This image was 512×512 in size. The following samples were chosen from the image,

(a)	Carports	12
(b)	Houses	10
(c)	Vegetation	9
(d)	Roads	8
(e)	Street with Car	5
(f)	Dry Land	3
(g)	Courts	2

a total of 49 samples belonging to 7 different classes. The test images in the 3 channels are depicted in Figs. 5.1, 5.2, and 5.3, respectively.

The second image was a high resolution thermal infra-red channel image, 512×512 in size. In this case only two classes: objects and background were considered. The sequence of operations performed on these images is described below.

The image to be analyzed was first studied carefully. Various samples belonging to different classes were selected. A good guess on the grid size was made after inspecting the sizes of the selected samples belonging to the object class. The shape, size, and orientation of the objects helped in selecting the

Figure 5.1: Channel 1 of the image – Visible range.

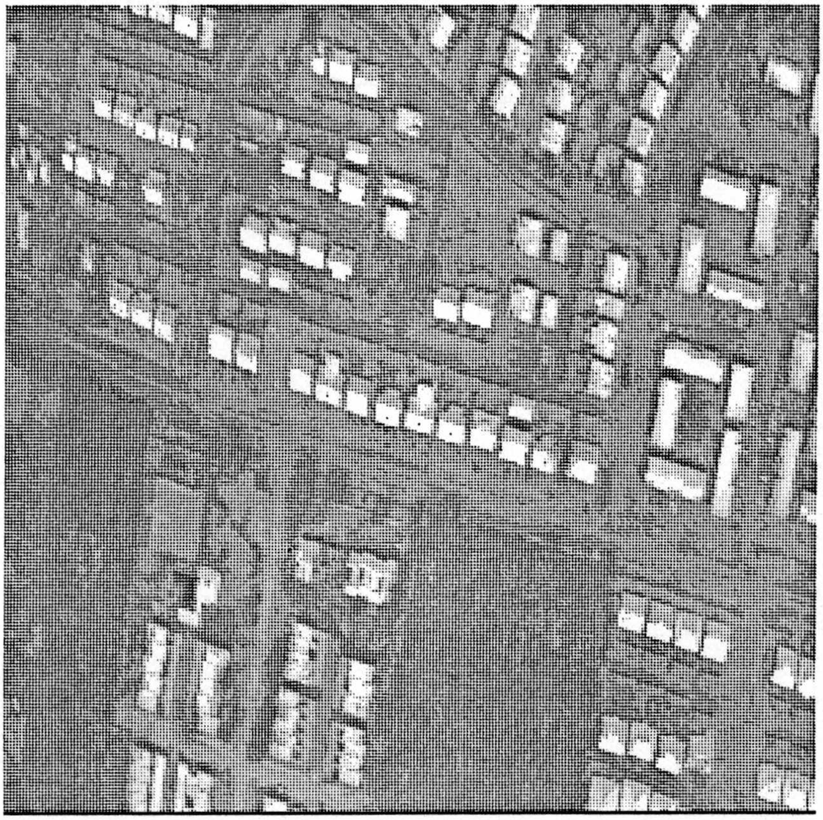

Figure 5.2: Channel 2 of the image – Thermal infra-red range.

Figure 5.3: Channel 3 of the image – Near infra-red range.

different intersample spacing distances (d) and the angular orientations (θ). After this step the entire image was subjected to the process of equal probability quantization (EPQ). As discussed earlier in chapter three, this is done to remove the effects of contrast and brightness variations in the image which might otherwise affect the measures extracted. The first order measures were computed from the quantized image. The GLC matrices were then extracted from the quantized image which acted as the input to the second order texture measure generation routine. For every combination of d and θ, six second order measures were generated. The measures were arranged as follows.

1. d_1, θ_1 : inertia, energy, entropy, local homogeneity, cluster shade, and cluster prominence.

2. d_2, θ_1 : same order of measures as above.

3. d_1, θ_2 : same order of measures as above.

4. d_2, θ_2 : same order of measures as above and so on.

This set of second order measures along with the first order measures formed the complete measurement set for the forward sequential search to operate upon. The forward sequential search and the Mahalanobis distance classifier formed the supervised part of the experiments. K-means was the unsupervised counterpart. A flow chart is shown on page 104 which illustrates the basic steps adopted in performing the experiments.

5.1.1 Experiments Performed on a High Resolution Multispectral Urban Scene Image

The image used for this part of the study was a multichannel image. The channels were analyzed individually and the results are discussed below.

Experiments Using Visible Channel Imagery

As indicated earlier 49 samples belonging to seven different classes were chosen. A 15×16 rectangular grid was chosen after studying the selected samples closely. Previous studies have indicated that typically the greater the number of values of δ, the better the discriminating power [1,4,11,15]. Practically speaking, these values should be limited and since no theoretical basis exists for the selection of δ, heuristics were employed. Earlier research efforts [3] have reported that in practice small values of intersample spacing distance (d) yield the best results. With these considerations in mind, the intersample spacing distances chosen were 1 and 3. Orientation of the streets and other objects accompanied by some heuristics compelled the angular orientations (θ) to be $339°, 79°$, and $25°$. Thus, six values of δ were chosen for this study,

1. $\delta_1 = (1, 339°)$,
2. $\delta_2 = (3, 339°)$,
3. $\delta_3 = (1, 79°)$,
4. $\delta_4 = (3, 79°)$,

5. $\delta_5 = (1, 25°)$,

6. $\delta_6 = (3, 25°)$.

After the selection of the samples, grid size, d's, and θ's the image was equal probability quantized (EPQ). The number of gray levels were reduced from 256 to 16. From the quantized image, the first order measures *viz.* mean and variance were computed for each of the 49 samples. The GLC matrices (16×16 in size) and the second order texture measures were computed from the quantized image for all the samples for each value of δ. The total number of measures under consideration was 36, since six measures were computed for six values of δ. These along with the first order measures formed a set of 38 measures for each of the 49 samples.

These measures were then subjected to the supervised and the unsupervised classification techniques. The experiments performed with the supervised statistical technique are described first.

The classification scheme was such that the classifier placed the samples into two categories – targets and background. Each time the algorithm was informed of the targets of interest and it did the rest *viz.* designing the classifier, testing it, selecting an optimal threshold, and computing the probability of error. Resubstitution method was the testing procedure employed. The classifier was designed (trained) with all the samples belonging to the target class and then tested with the complete set of samples.

Carports were the first targets considered. The forward sequential search algorithm picked up the following two measures.

1. Inertia ($d = 1, \theta = 79°$).

2. Energy ($d = 3, \theta = 339°$).

The classifier yielded a perfect classification, $POE = 0.0$. All the targets were correctly classified and no backgrounds were incorrectly assigned to the target class.

The next class of targets under scrutiny were the Houses. The following measures selected by the forward sequential search algorithm forced the statistical classifier to yield a correct classification.

1. Mean.

2. Cluster Prominence ($d = 1, \theta = 339°$).

3. Local Homogeneity ($d = 1, \theta = 339°$).

4. Entropy ($d = 1, \theta = 79°$).

Vegetative areas were the next considered targets. The forward sequential search algorithm came up with the following set of measures that resulted in an error-free classification.

1. Mean.

2. Inertia ($d = 1, \theta = 339°$).

The next targets of interest were the Roads. The statistical classifier isolated the roads correctly utilizing the following measures which the forward sequential search algorithm had selected.

1. Local Homogeneity ($d = 1, \theta = 339°$).

2. Mean.

3. Energy ($d = 1, \theta = 339°$).

4. Variance.

The Street with car samples were identified by the statistical classifier accurately, without any false alarms using the following 3 measures

1. Inertia ($d = 3, \theta = 79°$).

2. Mean.

3. Energy ($d = 1, \theta = 339°$).

Local Homogeneity ($d = 1, \theta = 79°$) was the measure that resulted in a perfect classification of the Dry land regions.

The statistical classifier used *variance* as the measure to detect the Courts in the image under consideration. The results discussed above are summarized in Table. 5.1.

Table 5.1: Results Obtained Using the Supervised Statistical Classification Technique (Visible Range).

Classes/ Number of Measures Used	*Verified Classificn.*	*Computer Classification*							*Accuracy*
		Cp	H	Veg	Roads	Swc	Dl	Crts	
Carports/2	12	12	0	0	0	0	0	0	100%
Houses/4	10	0	10	0	0	0	0	0	100%
Vegetation/2	9	0	0	9	0	0	0	0	100%
Roads/4	8	0	0	0	8	0	0	0	100%
Street with car/3	5	0	0	0	0	5	0	0	100%
Dry land/1	3	0	0	0	0	0	3	0	100%
Courts/1	2	0	0	0	0	0	0	2	100%
Total	49	-	-	-	-	-	-	-	-
Overall	-	-	-	-	-	-	-	-	100%

The results of the cluster analysis based classification technique are discussed next.

Carports were again considered first. Studying the measures for all the samples and inspecting the results obtained with the supervised technique, *inertia* ($d = 1, \theta = 79°$) was chosen as the measure. The K-means clustering algorithm was asked to cluster the samples into two clusters. A perfect classification resulted. No Carports were lost and no samples belonging to other classes were called targets.

Houses were considered next. The following measures resulted in a classification where two targets were lost and two samples belonging to the Dry land class were called targets, when the number of clusters requested was four.

1. Mean.

2. Inertia ($d = 1, \theta = 339°$).

Mean along with *inertia* ($d = 3, \theta = 339°$) resulted in a classification where three Houses were lost with no false alarms when the number of clusters was four.

Vegetation regions were the next set of targets under test. The measures

1. Mean.

2. Inertia ($d = 1, \theta = 339°$),

misclassified one target sample but encountered no false alarms when the number of clusters requested was seven.

Roads were the targets studied next. Two targets were lost and one Dry land, two Courts, and two Street with car samples were labelled targets. The number of clusters were five and the measures were

1. Mean.

2. Variance.

3. Entropy ($d = 1, \theta = 25°$).

4. Energy ($d = 1, \theta = 25°$).

This logically, was the best result among the many that were studied. This is indicated by the fact that Dry land and Street with car were classes not significantly different from the class under consideration.

Street with car was the next class under test. The following three measures resulted in the best classification where one target was lost while three Road samples and two Carports were labelled targets. The number of clusters was six.

1. Inertia ($d = 3, \theta = 79°$).

2. Mean.

3. Energy ($d = 1, \theta = 339°$).

Five clusters were needed with *local homogeneity* ($d = 1, \theta = 79°$) as the measure to provide a classification where all the targets (Dry land) were correctly classified while a House and a Vegetative region sample were picked up as targets.

Perfect classification resulted when Courts were the targets sought. The number of clusters was seven and the measures were

1. Variance.

2. Energy ($d = 1, \theta = 339°$).

3. Local homogeneity ($d = 1, \theta = 339°$).

4. Entropy ($d = 1, \theta = 339°$).

5. Inertia ($d = 1, \theta = 25°$).

The clustering algorithm did give rise to some false alarms, but logically speaking these samples were assigned to the best second choices (in most of the cases).

Table. 5.2 summarizes the results of the cluster analysis based (unsupervised) classification technique.

A Comparison of the Supervised and the Unsupervised Techniques

The major difference, besides the results was the fact that the supervised statistical classifier assigned class labels to the samples and as such in case of a miss it was easy to see the class to which the target was assigned. In case of the cluster analysis based classification technique, cluster assignments were made. In fact the target cluster was the only one that retained its identity. The rest of the samples were considered background and as such misses could not be interpreted.

To compare the performance of the two techniques a simple approach was adopted. Using the measures selected by the supervised technique, the response of the unsupervised technique was studied and vice-versa. Following are the results.

To isolate the Carports, the supervised technique picked up two measures as was indicated in the discussion above. These two measures were then used

Table 5.2: Results Obtained Using the Unsupervised Technique (Visible Range).

Classes/ Number of Measures Used	*Verified Classificn.*	*Cluster Analysis Results (Clusters)*							*Accuracy*
		Cp	H	Veg	Roads	Swc	Dl	Crts	
Carports/1	12	12	0	0	0	2	0	0	100%
Houses/2	10	0	8	0	0	0	1	0	80%
Vegetation/2	9	0	0	8	0	0	1	0	88%
Roads/4	8	0	0	0	6	3	0	0	75%
Street with car/3	5	0	0	0	2	4	0	0	80%
Dry land/1	3	0	2	0	1	0	3	0	100%
Courts/5	2	0	0	0	2	0	0	2	100%
Total	49	-	-	-	-	-	-	-	-
Overall	-	-	-	-	-	-	-	-	87.8%

for clustering. Perfect clusters resulted when the number of clusters requested was two. In fact, using *inertia* alone the clustering technique was able to correctly cluster the samples. However, when this measure (alone) was fed to the Mahalanobis distance classifier one target was lost.

Four measures were required by the supervised technique to discriminate between the Houses and rest of the samples. The unsupervised technique results were not so good using this set of measures. There were two sets of measures that yielded better but not perfect results. These sets of measures resulted in the loss of two targets each time, when fed to the Mahalanobis distance classifier.

Vegetative regions were easily detected using two measures by the supervised technique. These two measures resulted in the loss of one target sample when the unsupervised technique tried to cluster the samples into seven clusters. This in fact was the best result the clustering algorithm could provide.

Four measures were required to isolate the Roads from the other samples by the supervised technique. The unsupervised technique required a different set of four measures to yield a decent result. When fed to the Mahalanobis distance classifier, these measures resulted in the misclassification of three targets and falsely labelling one carport as a target.

The supervised and the unsupervised classification schemes used the same set of three measures when attempting to identify the Street with car samples in the image. The supervised technique yielded a perfect classification while the unsupervised technique encountered some errors (discussed above).

The supervised statistical classification technique provided a perfect classification using *local homogeneity* ($d = 1, \theta = 79°$) as the measure, while the cluster analysis based technique used the same measure to yield its best result – two false-alarms when Dry land samples were the targets sought.

One measure was required by the supervised scheme to identify the Courts in the image. This measure resulted in one Vegetative region sample and three Dry land samples being incorrectly called targets. Five measures were required by the unsupervised classification scheme to yield perfect classification for a total of seven clusters. These measures when fed to the Mahalanobis distance classifier resulted in a perfect classification.

Experiments Using Thermal Infra-red Channel Imagery

The same initial steps, as those in the previous case were employed. The same samples were retained and so were the other parameters *viz.* grid size, d's, and θ's. The image was quantized (16 gray levels) and the first order measures were extracted from it. A set of 36 second order texture measures were then computed and a series of experiments were performed. The results are discussed below, first for the supervised statistical classification technique.

Carports were considered first. The forward sequential search picked up *inertia* ($d = 3, \theta = 79°$) as the measure which resulted in a perfect classification.

Houses were the next set of targets. The classifier yielded an error free classification with *mean* as the measure, which was chosen by the forward sequential algorithm.

Vegetative regions were perfectly isolated using *mean* as the measure.

The following three measures were required to isolate the Roads from the rest of the samples.

1. Local Homogeneity ($d = 3, \theta = 25°$).

2. Mean.

3. Variance.

The statistical classifier needed three measures to identify the samples belonging to the Street with car class. The measures were

1. Cluster prominence ($d = 1, \theta = 339°$).

2. Mean.

3. Energy ($d = 1, \theta = 339°$).

Dry land regions were correctly classified, without any false-alarms using the following measures that were selected by the forward sequential search algorithm.

1. Cluster shade ($d = 1, \theta = 339°$).

2. Mean.

Mean was the only measure required to detect the Courts in the image. The results are tabulated in Table. 5.3.

Following are the results obtained from the unsupervised classification technique.

Carports were correctly isolated using the following measures

1. Mean.

2. Inertia ($d = 3, \theta = 79°$).

3. Inertia ($d = 3, \theta = 25°$).

Table 5.3: Results Obtained Using the Statistical Classification Technique (Thermal Infra-red Range).

Classes/ Number of Measures Used	*Verified Classificn.*	*Computer Classification*							*Accuracy*
		Cp	H	Veg	Roads	Swc	Dl	Crts	
Carports/1	12	12	0	0	0	0	0	0	100%
Houses/1	10	0	10	0	0	0	0	0	100%
Vegetation/1	9	0	0	9	0	0	0	0	100%
Roads/3	8	0	0	0	8	0	0	0	100%
Street with car/3	5	0	0	0	0	5	0	0	100%
Dry land/2	3	0	0	0	0	0	3	0	100%
Courts/1	2	0	0	0	0	0	0	2	100%
Total	49	-	-	-	-	-	-	-	-
Overall	-	-	-	-	-	-	-	-	100%

The number of clusters requested was two. These measures were chosen after experimenting with a lot of measures and different number of clusters.

The following measures provided a classification where only one House (target) was lost while no false alarms were encountered. The number of clusters was six.

1. Mean.

2. Local Homogeneity ($d = 3, \theta = 79°$).

With a request of three classes and *mean* as a measure, all the Vegetative regions were perfectly classified.

Roads posed some problems before a decent classification resulted. The number of clusters requested was seven and the measures were

1. Inertia ($d = 3, \theta = 25°$).

2. Local Homogeneity ($d = 1, \theta = 339°$).

3. Mean.

The classification resulted in one target sample being lost. This could be due to the fact that the class – Street with car – was not drastically different from the one under consideration and also some of the Dry land samples were reasonably like the targets sought.

Cluster shade ($d = 1, \theta = 25°$) was the measure that yielded the best classification for the Street with car samples – loosing one target and labelling three Vegetative region samples as targets. The number of clusters was six.

One Dry land region was lost while two Houses, one Road and one Street with car sample was incorrectly assigned to the target (Dry land) cluster. The number of clusters was seven and the measures were

1. Cluster shade ($d = 1, \theta = 339°$).

2. Local homogeneity ($d = 1, \theta = 339°$).

Two measures were required to classify the Courts correctly. The number of clusters was seven and the measures were

1. Mean.

2. Inertia ($d = 1, \theta = 339°$).

The results are tabulated in Table. 5.4.

Table 5.4: Results Obtained Using the Unsupervised Technique (Thermal Infra-red Range).

Classes/ Number of Measures Used	*Verified Classificn.*	*Cluster Analysis Results (Clusters)*							*Accuracy*
		Cp	H	Veg	Roads	Swc	Dl	Crts	
Carports/3	12	12	0	0	0	0	0	0	100%
Houses/2	10	0	9	0	0	0	2	0	90%
Vegetation/1	9	0	0	9	0	3	0	0	100%
Roads/3	8	0	0	0	7	0	1	0	87.5%
Street with car/1	5	0	0	0	0	3	1	0	60%
Dry Land/2	3	0	0	0	0	0	2	0	67%
Courts/2	2	0	0	0	0	0	0	2	100%
Total	49	-	-	-	-	-	-	-	-
Overall	-	-	-	-	-	-	-	-	89.8%

A Comparison of the Supervised and the Unsupervised Techniques

As explained earlier for the unsupervised classification scheme, interpretation of the misses was not possible since only the target cluster retained its identity. The approach described earlier was adopted for all the experiments to study the two techniques.

The supervised technique needed one measure to classify the Carports correctly without any false alarms. This measure resulted in one target being lost when clustering for two clusters. The unsupervised technique required three measures to yield a perfect classification. The number of clusters was two. The Mahalanobis distance classifier was also able to correctly classify the Carports using the three measures the unsupervised technique had used.

Mean was the measure used by the supervised technique to identify the Houses in the image. The unsupervised technique missed two Houses when attempting to cluster the samples into five clusters using *mean*. Another measure was required in addition to the *mean* for the unsupervised technique to yield its best result *viz.* the loss of only one target. These two measures resulted in a perfect classification when utilized by the statistical classifier.

Both the supervised and the unsupervised techniques were successful in isolating the Vegetative regions using *mean* as the measure. The number of clusters for the unsupervised technique was three.

Roads were discriminated from rest of the samples by the supervised technique with the help of three measures. The unsupervised technique required a different set of three measures to yield a classification where only one target was lost. The measures selected by the supervised technique resulted in the loss of two targets when clustering was attempted for seven clusters. For the same number of clusters, the other set of measures resulted in the loss of only one target sample. The Mahalanobis distance classifier yielded a perfect classification using the measures provided by the unsupervised technique.

The measures chosen by the forward sequential search algorithm did not yield good clusters when Street with car samples were sought. Similarly, the measure that produced decent clusters resulted in an extremely bad classification accuracy when the Mahalanobis distance classifier attempted to perform the classification.

Dry land samples were the next set of targets considered. The measures that provided a perfect classification for the supervised statistical technique failed to yield good clusters. The two measures that produced good clusters resulted in one Vegetative region and two Street with car samples to be labelled targets, when used by the Mahalanobis distance classifier.

Courts were easily identified by both the classification techniques. One Carport was assigned to the target cluster when clustering was attempted using the measures provided by the forward sequential search algorithm. The measures that yielded perfect clusters when used by the supervised classifier resulted in an error free classification.

Experiments Using Near Infra-red Channel Imagery

The same initial procedure was adopted as in the previous two cases. The results of the (statistical) technique are discussed below.

Carports were easily separated from the rest of the samples. The measure picked up by the forward sequential search algorithm –*variance*– resulted in a perfect classification.

The first order measures –*mean* and *variance*– were sufficient to discriminate between Houses and the rest of the samples.

The following two measures were selected by the forward sequential search to yield a perfect classification of the Vegetative regions.

1. Mean.

2. Inertia ($d = 1, \theta = 339°$).

Roads were the next targets considered. The forward sequential search algorithm and the Mahalanobis distance classifier could not yield a perfect classification. The following measures resulted in two of the targets being lost.

1. Mean.

2. Energy ($d = 3, \theta = 79°$).

As discussed earlier the samples of this class were not markedly different from some of the background classes, however only two samples were lost and assigned to the class –Street with car– which indeed is a valid second choice.

Only one measure – *cluster prominence* ($d = 3, \theta = 339°$) was needed by the statistical classifier to isolate Street with car samples from the rest.

Three measures

1. Cluster shade ($d = 1, \theta = 339°$).

2. Mean.

3. Local homogeneity ($d = 3, \theta = 339°$).

were required for the identification of Dry land samples in the image.

Cluster prominence ($d = 1, \theta = 339°$) was the measure that resulted in an error free classification when Courts were the targets sought. Table. 5.5 summarizes the results.

The results obtained from the cluster analysis based classification technique are discussed next.

With *variance* as the measure and a request of three clusters, the clustering algorithm presented clusters where Carports were separated from the rest of the samples.

Houses were considered next. The following set of measures resulted in a classification where only one target sample was lost. The number of clusters was five.

1. Inertia ($d = 1, \theta = 79°$).

2. Inertia ($d = 3, \theta = 79°$).

Table 5.5: Results Obtained Using the Statistical Classification Technique (Near Infra-red Range).

Classes/ Number of Measures Used	*Verified Classificn.*	*Computer Classification* Cp	H	Veg	Roads	Swc	Dl	Crts	*Accuracy*
Carports/1	12	12	0	0	0	0	0	0	100%
Houses/2	10	0	10	0	0	0	0	0	100%
Vegetation/2	9	0	0	9	0	0	0	0	100%
Roads/2	8	0	0	0	6	0	0	0	75%
Street with car/1	5	0	0	0	0	5	0	0	100%
Dry land/3	3	0	0	0	0	0	3	0	100%
Courts/1	2	0	0	0	0	0	0	2	100%
Total	49	-	-	-	-	-	-	-	-
Overall	-	-	-	-	-	-	-	-	95.9%

3. Local Homogeneity ($d = 3, \theta = 25°$).

4. Mean.

Six clusters were required for the classification of the Vegetative regions. One target sample was lost while no false alarms were noticed. The measures were

1. Inertia ($d = 3, \theta = 25°$).

2. Energy ($d = 1, \theta = 339°$).

3. Variance.

4. Mean.

One target sample (Roads) was lost while three background samples were incorrectly labelled targets when the following set of measures were used to isolate the roads. The clusters were six in number.

1. Inertia ($d = 3, \theta = 25°$).

2. Energy ($d = 1, \theta = 339°$).

3. Mean.

One sample belonging to the class –Street with car– and two Dry land samples were the ones which caused the false alarms. The samples were assigned to valid second choices as was evident from the image.

One target (Street with car) was lost when clustering was performed using *cluster prominence* ($d = 3, \theta = 339°$) as the measure and the number of clusters was six.

One Dry land sample was lost and two Road samples along with one Street with car sample were assigned to the Dry land cluster when the number of clusters was seven and the measures were

1. Cluster shade ($d = 1, \theta = 339°$).

2. Mean.

3. Local homogeneity ($d = 3, \theta = 339°$).

Two Vegetative regions were called Courts (targets) when clustering was performed using the following measures for a total of seven clusters.

1. Variance.

2. Mean.

Table. 5.6 summarizes the results.

A Comparison of the Supervised and the Unsupervised Techniques

Carports were easily separated from the rest of the samples by both the techniques using *variance* as the measure. The number of clusters in the unsupervised case was three.

Mean and *variance* were required by the supervised technique to isolate the Houses. Two houses were lost when the unsupervised technique tried to cluster the samples into five clusters using these measures. Four measures and five clusters were required by the clustering algorithm to yield a classification where only one target was lost. The Mahalanobis distance classifier could not yield a perfect classification using the measures preferred by the unsupervised technique.

Two measures were all that was needed by the supervised technique to detect Vegetative regions. These measures did not let the unsupervised technique cluster the samples into error free clusters. Instead, a set of four measures were required by the clustering routine to cluster the samples into six clusters with

Table 5.6: Results Obtained Using the Unsupervised Technique (Near Infra-red Range).

Classes/ Number of Measures Used	*Verified Classificn.*	*Cluster Analysis Results (Clusters)*							*Accuracy*
		Cp	H	Veg	Roads	Swc	Dl	Crts	
Carports/1	12	12	0	0	0	0	0	0	100%
Houses/4	10	0	9	0	0	0	0	0	90%
Vegetation/4	9	0	0	8	0	0	0	2	88.9%
Roads/3	8	0	0	0	7	0	2	0	87.5%
Street with car/1	5	0	0	0	1	4	1	0	80%
Dry Land/3	3	0	0	0	2	0	2	0	66.7%
Courts/2	2	0	0	0	0	0	0	2	100%
Total	49	-	-	-	-	-	-	-	-
Overall	-	-	-	-	-	-	-	-	89.8%

minimum error – loss of one target. Perfect classification resulted when the Mahalanobis distance classifier attempted to classify the samples using these measures.

The supervised technique could not yield a perfect classification of the Roads. The best results were achieved using two measures. These measures produced highly error prone clusters when clustering the samples. A set of three measures were required by the unsupervised technique to yield a decent classification for six clusters. Two targets were lost and two background samples were incorrectly labelled targets when the Mahalanobis distance classifier used the measures indicated by the unsupervised technique.

Both the classification techniques easily picked up the Street with car samples. The same measure proved useful in both the cases. However, one target was lost when clustering was attempted while no errors were encountered for the supervised statistical classification scheme.

Dry land samples were easily separated from the rest by the supervised technique while the unsupervised scheme failed to do so. The best results it produced were using the measure indicated by the supervised scheme.

Extremely bad clusters were formed when the measure provided by the measurement selection algorithm was used for clustering. Two measures were required for the unsupervised (cluster analysis based) technique to perfectly identify the Courts in the image. The Mahalanobis distance classifier also yielded a perfect classification using the measures indicated by the unsupervised technique.

From the individual analysis of the channels the following conclusions can be drawn.

Carports were easily identified by the statistical classification technique in all the channels. However, channels 2 and 3 required only one measure where as channel 1 needed two measures to yield a perfect classification. The cluster analysis based classification technique used three measures to produce perfect clusters in channel 2. In channels 1 and 3, only one measure was required to isolate the Carports from the other samples. Thus for the Carports channels 2 and 3 for the supervised classification technique, and channels 1 and 3 for the cluster analysis based technique provided the best classification.

Channel 2 provided the best results for the statistical classification technique as well as the unsupervised classification technique for the target class Houses. Channel 3, in case of the unsupervised technique provided the same accuracy but required more number of measures.

Vegetative regions were easily identifiable in channel 2 for both the classification techniques. Channel 2 also provided the best results for both the classification techniques when Roads were the targets under consideration.

Street with car samples presented some difficulty in channels 1 and 2, while in channel 3 only one target was lost. The noticeable fact was that, these samples were never correctly classified by the cluster analysis based classification scheme. This could be due to the fact that Roads and Dry land samples were not all that much different from the samples of this class. The supervised technique yielded perfect classification in each channel requiring only one measure in channel 3.

The supervised technique classified the Dry land samples correctly in each of the channels. The number of measures required was smaller (one) in channel 1. The cluster analysis based classification technique failed to yield good results. From the number of false-alarms point of view, it performed best in channel 1.

The supervised statistical and the unsupervised techniques yielded 100%

classification accuracy when Courts were being sought. Channel 2 seemed to be the best since the number of measures was fewer here. Thus overall channel 2 yielded the best results.

In the next section experiments performed on a high resolution single channel image are discussed. In this section and the next one there is no special section devoted to the comparison between the supervised and the unsupervised techniques as was done here, but the comparison can be found as one proceeds with the discussion.

5.1.2 Experiments Performed on a High Resolution Thermal Channel Image

The image under consideration for this part of the experiment was a single channel image 512×512 in size. It was inspected closely and 12 target and 30 background samples were chosen. The background samples were selected from different regions in the image to enhance the variety of such samples. A 14×14 square grid was chosen to be placed on the samples. This size was selected after inspecting the target samples in the image. The intersample spacing distances chosen were 2 and 5, while the angular orientations were 90° and 45°. Thus four values of δ were considered.

1. $\delta_1 = (2, 90°)$,

2. $\delta_2 = (5, 90°)$,

3. $\delta_3 = (2, 45°)$,

4. $\delta_4 = (5, 45°)$.

The image was equal probability quantized reducing the number of gray levels from 256 to 16. The first order measures were computed for each of the 42 samples, from the quantized image. Clustering was attempted using these measures. With *mean* as the measure two targets were misclassified and five background samples were incorrectly labelled targets. Five targets were lost and 13 background samples were wrongly classified when *variance* was used. In both the cases, the number of clusters requested was two. This was an attempt to study the effect of the first order measures on the cluster analysis based classification technique.

GLC matrices (16×16 in size) and subsequently the second order measures were computed from the quantized image. Since the number of values of δ was four, the total number of second order measures were 24 (six for each δ). These measures were then made available to the forward sequential search algorithm. This was an attempt to study the effects of second order measures on the supervised classification scheme. The following measures were selected by the algorithm that resulted in a POE of 0.0 *i.e* perfect classification,

1. Cluster Shade ($d = 5, \theta = 45°$).

2. Inertia ($d = 5, \theta = 45°$).

3. Inertia ($d = 5, \theta = 90°$).

4. Inertia ($d = 2, \theta = 90°$).

As a means of comparison of the two techniques, the measures selected by the supervised technique were used for clustering (unsupervised technique). In this case, one target and 13 background samples were misclassified.

When both, the first and the second order measures were used, the forward sequential search algorithm picked up the same set of measures as above. This indicated that no better clustering results could be expected with the help of the supervised technique. Various sets of measures were used for the unsupervised technique, but the clustering results were far from desired. Some of the results were

1. Measures selected

   - Mean.
   - Cluster Shade ($d = 5, \theta = 45°$).
   - Inertia ($d = 5, \theta = 45°$).

   One target was misclassified and 17 background samples were labelled targets.

2. Measures selected

   - Mean.
   - Inertia ($d = 5, \theta = 45°$).

Three targets and eight background samples contributed to the error.

In each case the number of clusters requested was two. No better results were obtained by changing the number of clusters. The measures were selected by inspecting the measures of all the samples along with some influence from the results obtained by the supervised technique.

The inability to arrive at good results forced us to reconsider the choices of the various parameters *viz.* the grid size, d's and the θ's. A lot of background area around the target was enveloped within the grid of size 14×14 and as such the reduction of the grid size was the primary thought. The size was reduced to 11×11. The first order measures were computed for all the 42 samples and used for clustering.

With *mean* as the measure, the clustering accuracy improved significantly. Only one target was misclassified and two background samples were mistaken to be targets. The *variance* did not improve upon this result.

Second order measures were then generated for all the samples with a grid size of 11×11. The d's were changed to 1 and 3, while the θ's were still 90° and 45°. These measures were then forwarded to the forward sequential search algorithm which picked up the following measures for a perfect classification.

1. Local Homogeneity ($d = 1, \theta = 90°$).

2. Cluster Prominence ($d = 1, \theta = 90°$).

Clustering with these measures, the algorithm misclassified four targets and two background samples were falsely called targets. *Mean* was added to the above set of measures, but the clusters did not change. With *mean* and *local homogeneity* ($d = 1, \theta = 90°$) the clusters were such that, again one target sample was lost while two background samples were called targets. Various combinations of measures were tried but at no time were the results as good as the ones indicated above. The number of clusters was two for most of the experiments and changing them did not produce better results.

It was evident from the results that for a θ of 90°, the results were much better than for a θ of 45°. A decision was then made to drop the measures corresponding to $\theta = 45°$ and generate those for $\theta = 0°$. This was promptly done and the entire set of 26 measures was subjected to the statistical classification technique. The following two measures yielded an error free classification,

1. Mean.

2. Inertia ($d = 1, \theta = 0°$).

These measures were then utilized by the unsupervised technique. When two clusters were requested, all the targets were correctly classified while two background samples created the false alarm. Only target sample was lost with no false alarms reported for three clusters.

Two new background samples were added to the set of the samples. The same measures discussed above were used and the same clustering accuracy resulted *i.e* one target misclassified. To test the robustness of the system a few more background samples were added to the set. The results are discussed below.

Six more samples were added to the set making the number of background samples 38 as against 12 samples belonging to the target class. The forward sequential search and the classifier could not yield a perfect classification. The best they could provide was a POE of 0.04. The measures were

1. Mean.

2. Local Homogeneity ($d = 1, \theta = 90°$).

These measures, while clustering, misclassified one target and incorrectly labelled five background samples as targets. The number of clusters was two. When *mean* and *inertia* ($d = 1, \theta = 0°$) were used for clustering, only target was lost while one background sample had an erroneous classification. Number of clusters under consideration was four. These measures, when used for classification by the Mahalanobis distance classifier provided the same POE as it did using the measures selected by the forward sequential search.

Four more background samples were appended to the set of samples. The number of background samples increased to 42, while the number of targets remained 12. The statistical classifier resulted in a perfect classification using the following measures chosen by the forward sequential search algorithm.

1. Local Homogeneity ($d = 1, \theta = 90°$).

2. Cluster Prominence ($d = 1, \theta = 90°$).

3. Mean.

4. Inertia ($d = 3, \theta = 0°$).

These measures when fed to the clustering algorithm resulted in the loss of five targets and a misclassification of five background samples. The number of clusters was two. For three clusters and the set of measures, which by now was convincingly powerful – *mean* and *inertia* ($d = 1, \theta = 0°$) – the accuracy was remarkable. One target was missed while one background sample was picked up as a target by the clustering algorithm. Two targets were lost and 20 background samples were incorrectly called targets when these measures were used to cluster the samples into two clusters. The final result for three clusters is tabulated in Table. 5.7. The performance of the statistical classification technique is not tabulated, to recall it yielded a 100% classification accuracy.

Table 5.7: Performance of the System (Cluster Analysis Based Classification Scheme).

Verified	*Cluster Analysis Results*				
Classification	*Objects*	*Bkgnd 1.*	*Bkgnd 2.*	*Total*	*Accuracy*
Objects	11	1	0	12	91.7%
Bkgnd	1	19	22	42	97.7%
Total	12	20	22	54	
		Overall	*Accuracy*	-	96.3%

In the experiments described above the first order measures were arranged after the second order measures. This order was reversed to study the effect of such a reversal on the measurement selection process. Three measures were selected by the forward sequential search algorithm which resulted in one background sample being called a target. Resubstitution testing method was employed and the measures were

1. Mean.

2. Inertia ($d = 1, \theta = 79°$).

3. Cluster Shade ($d = 1, \theta = 339°$).

Jackknife testing procedure was then used for this image. Extensive experiments were performed on the other images and thus this procedure was not attempted there. The jackknifing capabilities existed but in order to reduce the computation expenses this procedure was utilized for this image only. Besides this testing procedure was not the main focus of this study. The 12 targets were divided into two groups of six each and the 42 background samples into two groups of 21 each.

The first set of six targets and 21 background samples were used to train the Mahalanobis distance classifier. The forward sequential search algorithm picked up two measures for a POE of 0.0 and a threshold of 3.7. The second set of six targets and 21 background samples were used to test the classifier. A perfect classification resulted for the measures and the threshold chosen in the training phase. The measures were

1. Mean.

2. Inertia ($d = 1, \theta = 79°$).

Then the roles of the training and the testing sets were reversed. This time the second set of six targets and 21 background samples were used for training the classifier. Two measures were picked up resulting in an error free classification. The threshold was 4.7 and the measures were

1. Inertia ($d = 3, \theta = 79°$).

2. Mean.

One background sample was incorrectly labelled a target when the classifier was tested using the first set of six targets and 21 background samples. Interesting is the fact that the sample that was misclassified was the one which resulted in an error when resubstitution was the testing procedure used. The result is summarized in Table. 5.8.

Table 5.8: Performance of the System (Supervised Statistical Classification Scheme Employing Jackknifing Testing Procedure).

Verified	*Computer Classificn.*			
Classification	*Objects*	*Bkgnd*	*Total*	*Accuracy*
Objects	12	0	12	100%
Bkgnd	1	41	42	97.7%
Total	13	41	54	
		Overall	*Accuracy*	98.1%

5.2 Experiments With Multichannel Imagery

Three sets of experiments were performed in this category. The image used in the first part of the experiments was a multichannel image and thus provided the right environment to be explored for this type of study.

For the first set of experiments 24 new samples – 12 belonging to the Roads category and 12 to the Dry land category – were chosen. These samples were visually indistinguishable in channels 2 and 3 and as such these were the channels chosen for this part of the study. The grid size was the same as before *i.e* 15×16, the d's were 1 and 3, and the θ's 339°, 79°, and 25°. The channels were individually analyzed using the GLC method (as applied to single channel images), the texture measures from the two channels were appended and used for the task of object detection, measures from the gray level difference histograms were generated for the two channels and appended and used to analyze the image, and finally the technique proposed by Rosenfeld *et al.*[2] was used to analyze the image. Only the statistical classification scheme was employed in each of the cases.

Following results were obtained when analyzing the two channels individually. In channel 2, two roads were classified as Dry land and one Dry land sample was called a road. The measures were

1. Energy ($d = 1, \theta = 79°$).

2. Mean.

3. Cluster Shade ($d = 3, \theta = 339°$).

Four roads were called Dry land samples and two Dry land samples were assigned to the roads category, in channel 3 with the following set of measures.

1. Local Homogeneity ($d = 1, \theta = 339°$).

2. Inertia ($d = 3, \theta = 339°$).

Thus the samples could not be correctly classified in either of the channels.

The measures used in the above experiment were appended for all the samples (from both the channels) and the following set of measures yielded a perfect classification.

1. Energy ($d = 1, \theta = 79°$) (channel 2).

2. Mean (channel 3).

3. Local Homogeneity ($d = 1, \theta = 79°$) (channel 2).

4. Variance (channel 3).

5. Cluster Prominence ($d = 3, \theta = 339°$) (channel 2).

6. Energy ($d = 1, \theta = 339°$) (channel 3).

Measures from the gray level difference histograms for both the channels were generated and appended. One road sample was called Dry land and one Dry land sample was called road with the following set of measures.

1. Angular second moment ($d = 1, \theta = 79°$) (channel 2).

2. Inverse difference moment ($d = 1, \theta = 79°$) (channel 2).

3. Contrast ($d = 3, \theta = 25°$) (channel 3).

4. Entropy ($d = 1, \theta = 79°$) (channel 2).

5. Contrast ($d = 1, \theta = 339°$) (channel 2).

6. Angular second moment ($d = 3, \theta = 339°$) (channel 3).

Nine measures were required to yield a classification where two Dry land samples were called roads by the technique proposed by Rosenfeld *et al.*[2] (2-d GLD). The measures were

1. Angular second moment ($d = 3, \theta = 25°$).

2. Angular second moment ($d = 3, \theta = 339°$).

3. Angular second moment ($d = 1, \theta = 339°$).

4. Inverse difference moment ($d = 3, \theta = 79°$).

5. Angular second moment ($d = 3, \theta = 79°$).

6. Contrast ($d = 1, \theta = 339°$).

7. Inverse difference moment ($d = 1, \theta = 339°$).

8. Contrast ($d = 3, \theta = 339°$).

9. Angular second moment ($d = 1, \theta = 25°$).

The results are summarized in Table. 5.9.

Thus, it can be seen that the technique of appending the measures yielded the best results in this case.

Table 5.9: Probability of error of the Various Techniques Used for Object Detection in Multichannel Imagery.

POE / Number of Measures Used				
Ch 2.	Ch 3.	GLC (append)	GLD (append)	2-d GLD
0.125/3	0.25/2	0.0/6	0.08/6	0.08/9

Inspired by the above results, the techniques discussed were used to perform image segmentation in multichannel images. The second set of experiments utilized the same set of samples as was done in the case of analysis of single channel images *i.e* the same 49 samples belonging to seven different classes. In addition to those samples six more samples were chosen belonging to the Dry land class making it a total of nine samples in that class and 55 samples overall. The d's were 1 and 3, while the θ's were 339°, 79°, and 25°. As discussed earlier this image was a three channel image, each channel being 512×512 in size. The data sets and their generation was explained while discussing the experiments performed on each channel separately. The technique proposed by Rosenfeld *et al.*[2] is feasible for two channels only and as such channels 1 and 2 were used. Supervised statistical classification technique was employed in each of the following cases.

The measures from the GLC matrices and the first order measures generated for all the samples in the two channels were appended.

Carports were easily isolated using *inertia* ($d = 3, \theta = 79°$) (channel 2) as the measure. *Mean* (channel 2) was enough to separate the Houses from the rest of the samples. The vegetative regions were correctly classified using the following set of measures

1. Mean (channel 1).

2. Inertia ($d = 1, \theta = 339°$) (channel 1).

The Dry land category could not be correctly isolated. The best the classifier performed was misclassifying two Dry land samples and labelling them as vegetative regions, and picking up one house as a Dry land sample. The measures used was *cluster shade* ($d = 3, \theta = 339°$) (channel 1). The roads were correctly classified without any false alarms using the following set of measures.

1. Local Homogeneity ($d = 3, \theta = 25°$) (channel 2).

2. Mean (channel 1).

3. Cluster Prominence ($d = 1, \theta = 3396\circ$) (channel 1).

Street with car samples were classified without any errors, the measures being

1. Inertia ($d = 3, \theta = 79°$) (channel 1).

2. Local homogeneity ($d = 3, \theta = 339°$) (channel 2).

Variance (channel 1) was the measure used by the statistical classifier to detect Courts in the image.

Measures from the gray level difference histograms were generated for all the samples in both the channels (channels 1 and 2) and then appended.

Contrast ($d = 3, \theta = 79°$) (channel 2) was the measure used to isolate the Carports correctly. Two measures were required by the statistical classifier to separate the Houses form the rest of the samples.

1. Angular second moment ($d = 1, \theta = 339°$) (channel 2).

2. Mean ($d = 1, \theta = 339°$) (channel 1).

The following four measures were needed to result in an error free classification when the targets considered were the vegetative regions.

1. Contrast ($d = 1, \theta = 339°$) (channel 1).

2. Inverse difference moment ($d = 1, \theta = 339°$) (channel 1).

3. Angular second moment ($d = 1, \theta = 79°$) (channel 1).

4. Angular second moment ($d = 1, \theta = 339°$) (channel 1).

Dry land category was correctly identified, without any false alarms using the following set of measures.

1. Angular second moment ($d = 1, \theta = 79°$) (channel 1).

2. Mean ($d = 1, \theta = 79°$) (channel 1).

3. Inverse difference moment ($d = 3, \theta = 339°$) (channel 1).

4. Contrast ($d = 3, \theta = 79°$) (channel 2).

5. Angular second moment ($d = 3, \theta = 339°$) (channel 1).

Three measures were required to identify the roads in the image.

1. Inverse difference moment ($d = 3, \theta = 25°$) (channel 2).

2. Mean ($d = 1, \theta = 339°$) (channel 1).

3. Entropy ($d = 1, \theta = 339°$) (channel 1).

Street with car samples were separated from the rest by the statistical classifier using the following three measures

1. Contrast ($d = 3, \theta = 79°$) (channel 1).

2. Angular second moment ($d = 3, \theta = 339°$) (channel 2).

3. Inverse difference moment ($d = 1, \theta = 339°$) (channel 1).

Contrast ($d = 1, \theta = 339°$) (channel 1) was the sole measure that was required by the classifier to detect the Courts in the image without any errors. Thus 100% classification accuracy resulted.

Rosenfeld's technique was the next one used. Four measures were required to isolate the Carports correctly.

1. Contrast ($d = 1, \theta = 79°$).

2. Inverse difference moment ($d = 1, \theta = 339°$).

3. Angular second moment ($d = 1, \theta = 79°$).

4. Angular second moment ($d = 1, \theta = 339°$).

Houses were identified using the following measures.

1. Angular second moment ($d = 1, \theta = 79°$).

2. Angular second moment ($d = 1, \theta = 339°$).

3. Inverse difference moment ($d = 1, \theta = 339°$).

4. Contrast ($d = 1, \theta = 79°$).

One vegetative region was incorrectly labelled Dry land and one Dry land sample was assigned to the target class when the vegetative regions were being considered as the targets. The measures used were

1. Contrast ($d = 3, \theta = 79°$).

2. Inverse difference moment ($d = 3, \theta = 339°$).

3. Angular second moment ($d = 1, \theta = 79°$).

4. Angular second moment ($d = 1, \theta = 339°$).

Seven measures were required to correctly classify the Dry land category without any false alarms. The measures were

1. Contrast ($d = 1, \theta = 339°$).

2. Angular second moment ($d = 1, \theta = 339°$).

3. Contrast ($d = 1, \theta = 79°$).

4. Angular second moment ($d = 3, \theta = 339°$).

5. Angular second moment ($d = 3, \theta = 25°$).

6. Inverse difference moment ($d = 1, \theta = 79°$).

7. Inverse difference moment ($d = 3, \theta = 339°$).

Roads were identified using the following set of measures,

1. Contrast ($d = 1, \theta = 339°$).
2. Angular second moment ($d = 1, \theta = 339°$).
3. Angular second moment ($d = 1, \theta = 79°$).
4. Inverse difference moment ($d = 1, \theta = 79°$).
5. Inverse difference moment ($d = 1, \theta = 339°$).

Three measures were required by the statistical classifier to separate the Street with car samples from the rest. The measures were

1. Angular second moment ($d = 1, \theta = 339°$).
2. Contrast ($d = 1, \theta = 79°$).
3. Contrast ($d = 1, \theta = 339°$).

The results are summarized in Table. 5.10. The 2-d GLD technique did not commit drastic errors, but the GLD (append) technique resulted in a 100% accuracy. Both the set of experiments performed above, indicate that the appending technique is indeed a strong one for object detection as well as image segmentation.

As is evident from the table, the appending technique performed the best. For

Table 5.10: Probability of error of the Various Techniques Used for Image Segmentation in Multichannel Imagery.

	POE / Number of Measures Used		
Classes	GLC (append)	GLD (append)	2-d GLD
Carports	0.0/1	0.0/1	0.0/4
Houses	0.0/1	0.0/2	0.0/4
Vegetation	0.0/2	0.0/4	0.03/4
Dry land	0.05/1	0.0/5	0.0/7
Roads	0.0/3	0.0/3	0.0/5
SWCars	0.0/2	0.0/3	0.0/3
Courts	0.0/1	0.0/1	0.0/1

the same classification accuracy the number of measures were fewer in the case of the appending techniques and it was the only one that provided a perfect classification. It should however, be noted that the number of measures selected should, in general be one–tenth of the number of samples. Cases where more than two or three measures are used cannot be assessed as reliable estimates.

The third part of the study describes an attempt to utilize all the information available from the three channels to perform the classification. The classifiers were not informed of the type of the image or the number of channels. The same 49 samples were used as in the case of single channel analysis. In each channel 38 measures were generated for each sample. The measures from channel 1, followed by channel 2 and channel 3 measures formed the complete data set for each sample. The total number of measures was thus 114. These measures were used by both the classification techniques, the results of which are discussed below. The gray level difference method was also used to analyze the multichannel image. A comparison of both the methods is included at the end of this section.

5.2.1 Gray Level Co-occurrence Method for Texture Analysis in Multispectral Images

Carports were considered first. The forward sequential search algorithm had a large set of measures to choose from and chose the following measure which provided an error free classification.

1. Inertia ($d = 3, \theta = 79°$) (channel 2).

Clustering with this measure resulted in the loss of one target with the number of clusters being two. When *inertia* ($d = 1, \theta = 79°$) (channel 1) was used for clustering perfect classification resulted for two clusters. This measure, however, did not yield a perfect classification when attempted by the Mahalanobis distance classifier. It misclassified a target sample. When the forward sequential search was asked to pick up five measures irrespective of the error, it picked up the following set of measures for a perfect classification.

1. Inertia ($d = 3, \theta = 79°$) (channel 2).

2. Mean (channel 1).

3. Energy ($d = 3, \theta = 339°$) (channel 1).

4. Inertia ($d = 1, \theta = 339°$) (channel 1).

5. Variance (channel 1).

The unsupervised technique also yielded perfect clusters using these measures. The number of clusters was two.

Vegetative regions were considered next. *Mean* (channel 2) yielded a correct classification when used by both the techniques. For the unsupervised technique the number of clusters was three.

Houses were the next on the list. The supervised technique used *mean* (channel 2) to isolate the Houses from rest of the samples. Clustering with this measure resulted in two of the Houses being misclassified. *Mean* (channel 2) and *mean* (channel 1) resulted in an error free classification with four clusters. These measures resulted in a POE of 0.0, when fed to the Mahalanobis distance classifier.

Roads were the set of targets considered, next. The following measures helped the supervised technique to correctly classify the samples.

1. Local Homogeneity ($d = 1, \theta = 339°$) (channel 1).

2. Mean (channel 2).

3. Mean (channel 1).

4. Variance (channel 1).

5. Inertia ($d = 1, \theta = 339°$) (channel 1).

These measures, however, refused to let the unsupervised technique form perfect clusters. The following measures, for seven clusters, yielded a perfect classification

1. Mean (channel 2).

2. Mean (channel 1).

3. Inertia ($d = 1, \theta = 339°$) (channel 1).

The Mahalanobis distance classifier misclassified two targets and picked up a Street with car sample and a Dry land sample as targets using the above measures.

Cluster prominence ($d = 3, \theta = 339°$) (channel 3) was the measure picked up by the forward sequential search algorithm, using which the statistical classifier yielded a perfect classification, when Street with car was the target class sought.

This measure when used for clustering resulted in the loss of one target sample, the number of clusters being six. Perfect clusters were formed when *cluster shade* ($d = 1, \theta = 25°$) (channel 2) was used along with the above measure. The number of clusters was six. The Mahalanobis distance classifier also yielded a perfect classification using the two measures.

Local homogeneity ($d = 1, \theta = 79°$) (channel 1) was the measure that resulted in a perfect classification of the Dry land samples. This measure did not yield good clusters. Two measures were required by the clustering algorithm to provide error free clusters. The number of clusters was six and the measures were

1. Mean (channel 2).

2. Mean (channel 1).

A perfect classification resulted when these measures were used by the Mahalanobis distance classifier.

Variance (channel 1) identified the Courts in the image rather easily. *Mean* (channel 2) and *inertia* ($d = 1, \theta = 339°$) (channel 2) yielded a perfect clustering accuracy for seven clusters. The Mahalanobis distance classifier also produced a perfect classification using these measures. The results of the two techniques are summarized in Table. 5.11 and Table. 5.12.

Table 5.11: Results Obtained Using the Statistical Classification Technique (GLC append).

Classes/ Number of Measures Used	*Verified Classificn.*	*Computer Classification*							*Accuracy*
		Cp	H	Veg	Roads	Swc	Dl	Crts	
Carports/1	12	12	0	0	0	0	0	0	100%
Houses/1	10	0	10	0	0	0	0	0	100%
Vegetation/1	9	0	0	9	0	0	0	0	100%
Roads/5	8	0	0	0	8	0	0	0	100%
Street with car/1	5	0	0	0	0	5	0	0	100%
Dry land/1	3	0	0	0	0	0	3	0	100%
Courts/1	2	0	0	0	0	0	0	2	100%
Total	49	-	-	-	-	-	-	-	-
Overall	-	-	-	-	-	-	-	-	100%

Table 5.12: Results Obtained Using the Unsupervised Technique (GLC append).

Classes/ Number of Measures Used	*Verified Classificn.*	*Cluster Analysis Results (Clusters)*							*Accuracy*
		Cp	H	Veg	Roads	Swc	Dl	Crts	
Carports/1	12	12	0	0	0	0	0	0	100%
Houses/2	10	0	10	0	0	0	0	0	100%
Vegetation/1	9	0	0	9	0	0	0	0	100%
Roads/3	8	0	0	0	8	0	0	0	100%
Street with car/2	5	0	0	0	0	5	0	0	100%
Dry land/2	3	0	0	0	0	0	3	0	100%
Courts/2	2	0	0	0	0	0	0	2	100%
Total	49	-	-	-	-	-	-	-	-
Overall	-	-	-	-	-	-	-	-	100%

The following comments are in order here. The supervised classification technique yielded a 100% accuracy and it had in fact done so for each of the channels (almost except for the roads category in the third channel) individually. The unsupervised technique had never enjoyed a 100% accuracy, but it did so now. This shows that measures from different channels when used together have a better discriminating power than those from a single channel only.

5.2.2 Gray Level Difference Method for Texture Analysis in Multispectral Images

An approach somewhat similar to the one just described was used. Measures were generated for each channel separately and then appended together as discussed above. The same d's and θ's were used to generate the GLC matrices as before and from these the absolute difference histograms were computed. Contrast, Angular Second Moment, Entropy, Mean, and Inverse Difference Moment were the measures computed from these histograms. Since six values of δ were considered and five measures for each δ, 30 measures per channel were under consideration. Appending all the channels made it a 49 sample 90 measure problem.

Carports were easily identified by the supervised technique using *contrast* ($d = 3, \theta = 79°$) (channel 2) as the measure. This was not at all surprising since *contrast* is analogous to *inertia* and the d, θ, and the channel number indicate that exactly the same measure was chosen as was in the case of the GLC's.

The unsupervised technique misclassified one target when clustering the samples into two clusters using these measures. *Contrast* ($d = 1, \theta = 79°$) (channel 1) correctly clustered the Carports separately from the other samples when two clusters were requested. The Mahalanobis distance classifier lost a Carport when using this measure for classification. *Inertia* ($d = 3, \theta = 79°$) (channel 2) and *inertia* ($d = 1, \theta = 79°$) (channel 1) helped both the techniques yield a perfect classification. The number of clusters for the unsupervised technique was two.

Houses were considered next. The supervised technique, with the following measures, isolated the Houses correctly,

1. Inverse Difference Moment ($d = 1, \theta = 79°$) (channel 3).

2. Inverse Difference Moment ($d = 1, \theta = 339°$) (channel 2).

The unsupervised technique did not encounter good success with these measures. Clustering the samples into five clusters with

1. Inverse Difference Moment ($d = 1, \theta = 79°$) (channel 3).

2. Inverse Difference Moment ($d = 1, \theta = 25°$) (channel 2).

3. Inverse Difference Moment ($d = 1, \theta = 339°$) (channel 1).

resulted in a perfect classification as did the Mahalanobis distance classifier.

Vegetative regions were discriminated from the rest by the supervised technique using

1. Mean ($d = 1, \theta = 79°$) (channel 3).

2. Mean ($d = 1, \theta = 339°$) (channel 1).

The clustering algorithm did not yield good results using these measures. In fact the best result it produced classified all the targets correctly and labelled one Dry land sample and a road sample as targets. The number of clusters was four and the measures were

1. Mean ($d = 1, \theta = 79°$) (channel 3).

2. Mean ($d = 1, \theta = 339°$) (channel 3).

These measures when fed to the Mahalanobis distance classifier resulted in the loss of a target and one Dry land sample and a road sample falsely being called targets.

Roads were easily isolated by the supervised technique using the following set of measures

1. Mean ($d = 1, \theta = 339°$) (channel 1).

2. Inverse Difference Moment ($d = 3, \theta = 25°$) (channel 2).

The unsupervised technique did not do well with these measures but provided a decent classification with the following set of measures

1. Inverse Difference Moment ($d = 3, \theta = 25°$) (channel 2).

2. Inverse Difference Moment ($d = 1, \theta = 339°$) (channel 2).

3. Inverse Difference Moment ($d = 1, \theta = 339°$) (channel 1).

Only one target was lost while no false alarms resulted. The number of clusters was five. The Mahalanobis distance classifier misclassified one target and incorrectly called two Carports as targets using these measures.

The following measures forced the statistical classifier to correctly classify the Street with car samples.

1. Inverse difference moment ($d = 3, \theta = 339°$) (channel 3).

2. Contrast ($d = 1, \theta = 339°$) (channel 1).

The cluster analysis based classifier failed to yield an error free classification using these measures. The following measures resulted in seven clusters where one target was lost and one vegetative region was incorrectly labelled target (Street with car).

1. Inverse difference moment ($d = 3, \theta = 339°$) (channel 1).

2. Inverse difference moment ($d = 3, \theta = 339°$) (channel 3).

The Mahalanobis distance classifier also misclassified a target sample while labelling one vegetative region as target using these measures.

Dry land samples were correctly isolated by the supervised classifier using *entropy* ($d = 1, \theta = 339°$) (channel 1) as the measure. The clustering algorithm labelled two Road samples as targets when clustering for six clusters using this measure. Perfect classification resulted when *entropy* ($d = 1, \theta = 339°$) (channel

2) was used along with the above measure. The number of clusters was seven. The Mahalanobis distance classifier also resulted in a perfect classification utilizing the two measures.

With *contrast* ($d = 1, \theta = 339°$) (channel 1) as the measure the Courts were identified without any error, by the supervised technique. However, a different measure was required by the unsupervised technique to result in a perfect classification. This measure also forced the Mahalanobis distance classifier to yield a perfect classification. The number of clusters for the unsupervised technique was seven and the measure was *angular second moment* ($d = 1, \theta = 79°$) (channel 1). The results are summarized in Table. 5.13 and Table. 5.14.

Table 5.13: Results Obtained Using the Statistical Classification Technique (GLD append).

Classes/ Number of Measures Used	*Verified Classificn.*	*Computer Classification* Cp	H	Veg	Roads	Swc	Dl	Crts	*Accuracy*
Carports/1	12	12	0	0	0	0	0	0	100%
Houses/2	10	0	10	0	0	0	0	0	100%
Vegetation/2	9	0	0	9	0	0	0	0	100%
Roads/2	8	0	0	0	8	0	0	0	100%
Street with car/2	5	0	0	0	0	5	0	0	100%
Dry land/1	3	0	0	0	0	0	3	0	100%
Courts/1	2	0	0	0	0	0	0	2	100%
Total	49	-	-	-	-	-	-	-	-
Overall	-	-	-	-	-	-	-	-	100%

Table 5.14: Results Obtained From the Unsupervised Technique (GLD append).

Classes/ Number of Measures Used	*Verified Classification*	*Cluster Analysis Results (Clusters)*							*Accuracy*
		Cp	H	Veg	Roads	Swc	Dl	Crts	
Carports/1	12	12	0	0	0	0	0	0	100%
Houses/3	10	0	10	0	0	0	0	0	100%
Vegetation/2	9	0	0	9	0	1	0	0	100%
Roads/3	8	0	0	1	7	0	0	0	87.5%
Street with car/2	5	0	0	0	0	4	0	0	80%
Dry land/2	3	0	0	1	0	0	3	0	100%
Courts/1	2	0	0	0	0	0	0	2	100%
Total	49	-	-	-	-	-	-	-	-
Overall	-	-	-	-	-	-	-	-	95.9%

5.2.3 A Comparison of GLC and GLD Methods

In the case of Carports, the two methods performed identically. The measure selected by the forward sequential search algorithm, when used for clustering, resulted in the loss of a target sample. The measure that yielded perfect clusters in the unsupervised technique forced the Mahalanobis distance classifier to loose a target. In fact, the measures used in both the methods were analogous to each other.

The accuracy was even in the case of Houses, too. The set of measures used were different and the number of clusters required was four in the case of the GLC method and five in the case of the GLD method. The GLD method required more measures to come up with the perfect clusters, in both the supervised and the unsupervised techniques.

The GLC method resulted in a better accuracy (unsupervised classification) for the next set of targets, *i.e* Vegetation. Two background samples were called targets in the GLD method – a Dry land sample and a road sample. The accuracy was the same for the supervised classification scheme.

For the next set of targets, *i.e* Roads, the number of measures required for perfect classification was more in the case of the GLC method (supervised technique) even though the accuracy was the same. For the unsupervised classification scheme, the GLC's yielded a better classification accuracy. The GLD method lost one sample without giving rise to any false alarms.

The samples belonging to the "Street with car" class were correctly identified by the supervised technique in both, the GLC based and the GLD based techniques. The unsupervised technique could perfectly classify the samples for the GLC based method but failed to do so for the GLD method.

The Dry land samples and Courts were classified without any errors by the supervised as well as the unsupervised classification schemes for both the GLC and GLD based methods.

Thus both the methods, GLC based and GLD based, provided 100% accuracy as far as the supervised classification was concerned. The GLC's performed better in the case of unsupervised scheme (100% accuracy). The fact should however be noted that the errors committed by the GLD method were not drastic and a few more δ considerations would probably have avoided them. The nature of the classes should also be kept in mind while assessing the relative superiority of one or the other method.

The flow chart of the typical sequence of operation is depicted on the following page.

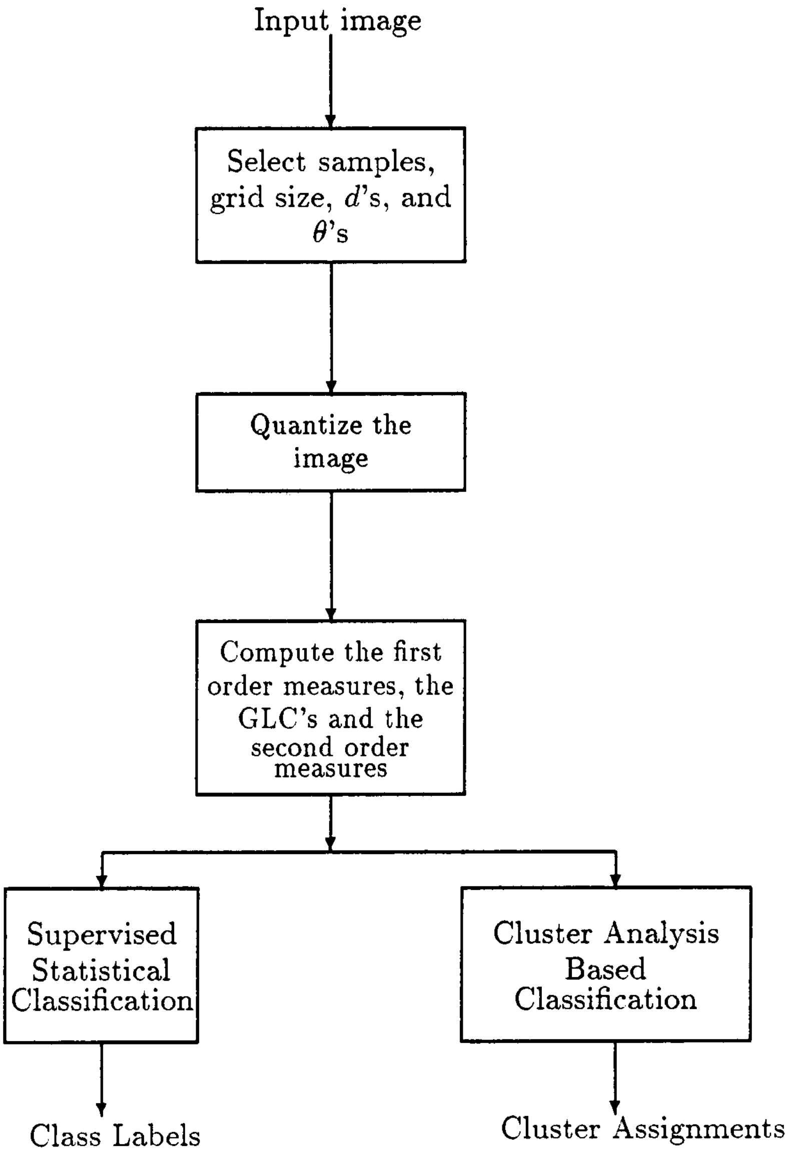

Figure 5.4: A flow chart of the typical sequence of operation.

CHAPTER 6

SUMMARY AND CONCLUSIONS

A GLC based texture analysis package useful for object detection and image segmentation was developed. Supervised statistical classification technique has been the main stay of many a research efforts. Difficulties in acquiring training samples and the high cost associated with it has forced the researchers to be on the look out for other classification techniques. Cluster analysis was the approach suggested here. It provides a logical means to perform unsupervised classification of the data in a d-dimensional space. Performance of both these techniques was studied for a wide variety of cases. Multispectral texture analysis has been a neglected field because of the extremely high cost associated with acquiring of the multispectral scanners. Rosenfeld *et al.*[2] proposed techniques to perform multispectral texture analysis, which were extensions of the techniques being used for the analysis of single channel imagery. Because of the shortcomings of these techniques when applied to a b-channel image, where $b > 2$, alternative strategies are sought. Multispectral texture, conceptually difficult to visualize, was discussed from the computational standpoint. Simple techniques based on the GLC method and the GLD method were suggested to perform texture analysis in multispectral images.

Various experiments were performed to study the performance of the different techniques discussed in this thesis. A high resolution multispectral urban scene image was the first image to be considered. This was a three channel image incorporating the visible, the thermal infra-red, and the near infra-red ranges. These channels were considered as subimages and dealt with independently when studying the performance of the classification techniques as applied to single channel imagery. The supervised statistical classification technique yielded a 100% classification accuracy when channels 1 and 2 were analyzed. In channel 3, the roads could not be perfectly isolated from the rest of the samples. This was because, the other classes – dry land and street with cars – were not drastically different from the targets being sought (roads). The unsupervised technique did not perform so well. Various sets of measures and different number of clusters were needed to experiment with before decent results were achieved. The main difference between the statistical classification scheme and the cluster analysis based classification technique was that the statistical classifier assigned class labels to the samples and as such it was easy to interpret the errors – misses and/or false alarms. The unsupervised technique yielded cluster assignments where only the target cluster retained its identity and as such the errors could not be interpreted. The background samples were arbitrarily assigned to the background classes and thus when a target was missed it was difficult to say which class it was assigned to.

A high resolution thermal infra-red channel image was the other image used in this study. The statistical supervised technique yielded a 100% clustering accuracy, while the cluster analysis based classifier was not far behind with a 96.3% classification accuracy. One target was lost and one background sample was picked up when the clustering program tried to cluster the samples into three clusters. Resubstitution and Jackknifing testing procedures yielded the same classification accuracy (98.1%) when the first order measures were arranged before the second order measures. Jackknifing testing procedure was not employed in any other case because this technique was not the main focus of this study and this technique is computationally expensive as compared to the resubstitution testing procedure.

Three sets of experiments were performed in the category of multispectral texture analysis. In the first set of experiments, 12 samples belonging to the roads class and 12 belonging to the dry land class were chosen. These samples were very much alike in the second and the third channel and as such these channels were utilized for this part of the study. These channels were individually analyzed using the GLC method and neither of them could successfully separate the samples. These measures were then appended in accordance with the approach suggested here and perfect classification resulted. This was because the forward sequential search algorithm picked up a set of measures which was a blend of the measures generated from both the channels. The measures generated from the difference histograms for both the channels were appended and subjected to the forward sequential search operation. One road was called a dry land sample and a dry land sample was called a road, when these measures were utilized by the statistical classifier. Rosenfeld's technique was the final approach tested on these samples. This technique labelled two dry land samples as roads. Thus the appending of the GLC based measures was the only technique that provided a perfect classification.

Thus the technique of appending measures from different channels performed well in the object detection domain. It yielded a 100% classification accuracy when utilized for the task of image segmentation. The same image (high resolution multispectral urban scene image) was used here. The same samples as in the case of individual channel analysis were used. In addition to these 6 samples were added to the dry land category making the total number of samples 55. Since Rosenfeld's technique was feasible only in case of 2 channels, channel 1 and channel 2 were used for this part of the study. Rosenfeld's technique performed fairly well here. When isolating vegetative regions this technique called 1 target a dry land sample and picked up 1 dry land sample as a vegetative region. The GLC appending technique had trouble isolating the dry land class. The GLD histogram based measures when appended yielded perfect results. Thus in both the cases discussed here, the technique of appending the measures provided the best results.

To study the relative performance of the two appending techniques – GLC based and GLD based, they were used to analyze all the 3 channels of the multichannel image. The GLC based technique performed better than the gray level difference based technique. The cluster analysis based classification technique yielded a 100% clustering accuracy, underlining the fact that analyzing multichannel images provides better results than analyzing just a single channel.

It is true that the technique of appending measures is not really performing multispectral texture analysis, but it is in fact texture analysis in multispectral images. Various aspects in this field need exploring. The concept of multispectral texture needs to be developed. A technique in accordance with the concept, which can practically be feasible needs to be devised.

BIBLIOGRAPHY

BIBLIOGRAPHY

[1] M. M. Trivedi and C. A. Harlow, "Identification of Unique Objects in High Resolution Aerial Images," *Optical Engineering*, vol. 24 No. 3, pp. 502–506, May/June, 1985.

[2] A. Rosenfeld, C. Wang, and A. Y. Wu, "Multispectral Texture," *IEEE Trans. Systems, Man and Cybernetics*, vol. SMC-12, No. 1, pp. 79–84, January/February, 1982.

[3] L. V. Gool, P. Dewaele, and A. Oosterlinck, "Texture Analysis Anno 1983," *Computer Vision, Graphics, and Image processing 29*, pp. 336–357, 1985.

[4] M. M. Trivedi, C. A. Harlow, R. W. Conners, and S. Goh, "Object Detection Based on Gray Level Cooccurrence," *Computer Vision, Graphics, and Image Processing 28*, pp. 199–219, 1984.

[5] M. M. Trivedi, C. A. Harlow, D. H. Cress, and C. Chen, "Detection of Objects in High Resolution Multispectral Aerial Images," *SPIE, Applications of Artificial Intelligence II*, vol. 548, pp. 258–262, 1985.

[6] M. M. Trivedi, C. Chen, and C. A. Harlow, "Detecting Objects in High Resolution Images," in *Proceedings of the Ninteenth Southeastern Symposium on Systems Theory*, (Clemson), pp. 23–26, March 1987.

[7] M. M. Trivedi and C. Chen, "Object Detection By Step-Wise Analysis of Spectral, Spatial, and Topographic Features," *Computer Vision, Graphics, and Image processing*, 1989.

[8] P. Dewaele, L. V. Gool, P. Wambacq, and A. Oosterlinck, "Texture Inspection with Self-Adaptive Filters," in *Proceedings of the Ninth International Conference on Pattern Recognition*, (Rome, Italy), November 1988.

[9] O. R. Mitchell, C. R. Myers, and W. Boyne, "A Max-Min Measure for Image Texture Analysis," *IEEE Trans. Computers*, pp. 408–414, April 1977.

[10] C. T. Ng, *A Structural Analysis of Periodic and Almost Periodic Textures.* Master's thesis, Dept. of Electrical Engineering, Louisiana State University, Baton Rouge, Lousiana, May 1984.

[11] R. W. Conners, M. M. Trivedi, and C. A. Harlow, "Segmentation of a High Resolution Urban Scene Using Texture Operators," *Computer Vision, Graphics, and Image processing 25*, pp. 273–310, 1984.

[12] C. A. Harlow, M. M. Trivedi, and R. W. Conners, "Use of Texture Operators in Segmentation," *Optical Engineering*, vol. 25 No. 11, pp. 1200–1206, November, 1986.

[13] L. H. Siew, R. M. Hodgson, and E. J. Wood, "Texture Measures for Carpet Wear Assessment," *IEEE Trans. Pattern Analysis and Machine Intelligence*, vol. 10, No. 1, pp. 92–105, 1988.

[14] S. J. Roan, J. K. Aggarwal, and W. N. Martin, "Multiple Resolution Imagery and Texture Analysis," *Pattern Recognition*, vol. 20 No. 1, pp. 17–31, 1987.

[15] J. S. Weszka, C. R. Dyer, and A. Rosenfeld, "A Comparative Study of Texture Measures for Terrain Classification," *IEEE Trans.on Systems, Man and Cybernetics*, vol. SMC-6, No. 4, pp. 269–285, April, 1976.

[16] R. W. Conners and C. A. Harlow, "A Theoretical Comparison of Texture Algorithms," *IEEE Trans. Pattern Anal. Mach. Intelligence*, vol. PAMI–2, No. 3, pp. 204–222, 1980.

[17] R. W. Conners and C. A. Harlow, "Towards a set of Structural Textural Analyzer Based on Statistical Methods," *Computer Vision, Graphics, and Image processing 12*, pp. 224–256, 1980.

[18] R. M. Haralick, K. Shanmugam, and I. Dinstein, "Textural Features For Image Classification," *IEEE Trans. Systems, Man and Cybernetics*, vol. SMC-3, pp. 610–621, November, 1973.

[19] J. T. Tou and R. C. Gonzalez, *Pattern Recognition Principles.* Massachusetts: Addison-Wesley Publishing Company, 1974.

[20] R. W. Conners and C. A. Harlow, "Equal Probability Quantizing and Texture Analysis of Radiographic Images," *Computer Graphics and Image Processing 8*, pp. 447–463, 1978.

[21] R. W. Conners and C. A. Harlow, "The Linear Distribution Function and Texture Analysis of Radiographic Images," Tech. Rep., Image Analysis Lab, Bioengineering/ Advanced Automation Program, University of Missouri-Columbia, Columbia, Missouri, May 1976.

[22] M. M. Trivedi and J. C. Bezdeck, "Low-Level Segmentation of Aerial Images with Fuzzy Clustering," *IEEE Trans. Systems, Man and Cybernetics*, vol. SMC-16, No. 4, pp. 589–597, July/August, 1986.

[23] R. O. Duda and P. E. Hart, *Pattern Classification and Scene Analysis.* John Wiley and Sons, 1973.

[24] R. C. Gonzalez and P. Wintz, *Digital Image Processing, second edition.* Addison-Wesley Publishing Company, 1987.

VITA

Amol G. Bokil was born in Bombay, India on July 31, 1964. He attended Kendriya Vidyalaya (Central School), Colaba and graduated with honors in 1979. After successfully completing a two year junior college course at Elphinstone College, Bombay he joined the S.D.M college of Engineering and Technology, Dharwar (affiliated to Karnatak University). In 1985 he graduated with a Bachelor of Engineering (B.E) degree in Electronics and Communication Engineering. He secured second rank in the entire Karnatak University at the final year B.E examination. He was employed by the S.D.M college of Engg. and Technology, Dharwar in the capacity of a lecturer, between July 1985 and August 1986.

In September 1986, the author began his study toward a Master of Science in Electrical Engineering, at the University of Tennessee, Knoxville. He was a teaching and a research assistant since June 1987, the research being concentrated in the area of Computer Vision and Pattern Recognition.

The author is a member of Tau Beta Pi and the IEEE societies.